**REPLY TO #1 REFEREE'S QUERIES AND DESCRIPTION OF CHANGES DONE FOLLOWING HER/HIS SUGGESTIONS**

Many thanks for your valuable comments and suggestions than helped us to improve the quality of the manuscript. As you will see we took into account all your comments when reviewing the new version.

1.) **My first comment is related to the definition of primary aerosol particles in an urban location. A quite large part of the Introduction is spent on what fractions have been primary particles and originating from NPF in earlier studies in urban environments. Furthermore, since you claim that you can distinguish NPF events from primary emissions in this study, I think it should be more clear exactly how you define these two processes. In the Introduction, in lines 18-20 on page 2, you discuss production mechanisms of ultrafine particles from traffic: "condensation of semi-volatile phases vapor species that creates new UFP during dilution and cooling of engine exhaust emissions near the source". After that you write "most studies consider them as primary", "or quasi-primary particles". How do you define these particles, that form by nucleation in the tailpipe or a second after exiting? I guess you define them as primary, but I think that should be clear.**

We agree. It was not enough clear. We also define such particles as primary ones. The quoted paragraph has been rewritten as follows:

*In urban areas, traffic emissions are a major source of UFP (Kumar et al., 2014; Ma and Birmili, 2015; Pey et al., 2008; Pey et al., 2009; Dall'Osto et al., 2012; Salma et al., 2014; Paasonen et al., 2016). These emissions include primary UFP exhaust emissions (Shi and Harrison, 1999; Shi et al., 2000; Charron and Harrison, 2003; Uhrner et al., 2012); cooling of engine exhaust emissions and condensation of semi-volatile phases vapor species that creates new UFP during dilution (Charron and Harrison, 2003; Kittelson et al., 2006; Robinson et al., 2007; Rönkkö et al., 2017). These are also considered primary particles, since they are formed near the source.*

2.) **Comment 1) leads to the question how you know that the regional NPF events are not "primary aerosol particles" formed by nucleation in the tailpipe or soon after exiting. Such emissions of 6-11 nm particles (Kittelson et al., 2006) dominate the number emissions. Furthermore, such emissions from thousands of cars in the Madrid area would likely look like a regional NPF event, since the emitted particles will grow by condensation in the atmosphere. One argument against this hypothesis, that the particles are primary, is the fact that your formation rates and number concentrations of 9-25 nm particles peak at noon when BC levels are at minimum. On the other hand, condensational growth is strongest at noon or in the afternoon since photochemical production of condensable vapors is dependent on solar radiation. Therefore, even though primary emissions are likely highest in the morning and evening rush hours, the likeliness that the emitted nano-particles grow into the 9-25 nm interval (which you refer to as ultrafine particles and for which you present the diurnal cycle in Fig. 5a) may be highest at noon or in the afternoon. I think you need to strengthen your arguments and definitions here when you refer to the events as "regional NPF events". Also, could you add diurnal cycles of number concentrations associated with the PSM data to Fig. 5a?**

We consider regional NPF events days in which the particle size distributions at all our stations have the same evolution. Being these stations 17 km apart and being all of them of different categories (urban, urban background and suburban), we assume that the particles are not formed in the tailpipe, i.e., they are not primary. Otherwise there would be significant differences when comparing the PSD at the suburban station, which is not highly influenced by traffic, as opposed to the urban station. Another argument is the fact that particle concentrations measured with the PSM are higher in the suburban station, compared with the urban station (as shown in Fig S7). Additionally, PSM data show an increment in the concentration of all size ranges around the same time in which we begin to see growth in the SMPS size distributions, meaning that these particles started growing from 1.2 nm, therefore they are not 6-11 nm emissions as suggested. Dall'Osto et al. (2013) characterized at regional scale (40 km) the simultaneous occurrence of these photochemical nucleation events covering vast zones with very high nucleation. Because it was not clearly augmented, the following text was modified to clarify this question:

*In the selected episodes, intensive daytime nucleation and subsequent condensational growth processes took place simultaneously at urban and suburban stations, located 17 km apart, and accordingly we classify these as regional NPF episodes. Being all stations differently influenced by traffic (influenced, slightly and not influenced by traffic), we can affirm that these episodes are regional events and not representative of primary emissions. Otherwise, we would observe significant differences at our stations. Additional arguments are the fact that number concentrations of sub-25 nm particles peak at noon, when BC levels are at their minimum, as well as higher concentration of particles measured by PSM at the suburban station, compared to the urban station, implying that the particles are not originated from traffic sources.*

Fig. 5 (now Fig. 3) has been modified to include PSM data, as suggested by both referees. We agree that this figure was necessary. Now we see the 3 peaks, 2 from traffic and the midday one.

**3.) Following up on Comment 2), in Sect. 3.2.1 you equate the occurrence of "10 nm particles" with NPF. Could these particles not just as well be primary?**

See reply to Comment 2).

**4.) Page 5, lines 22-23: Why did you choose the number concentration in the 9-25 nm interval in Eq. 4 for your definition of the formation rate? Why do you not use your PSM data for the formation rates?**

We chose this size interval (9-25 nm) due to the detection limit of the SMPS, which is the instrument we used to calculate growth rates, sinks and formation rates. PSM data was very noisy and we preferred not to use it for this purpose. However, following both Referees' comments, the calculations have been made again using PSM data. Figure 6 and previous results using SMPS have been removed, and GR calculated with PSM data and $J_1$ results and discussion have been provided:

*Growth rates ($GR_{PSM}$) and total formation rates of 1.2-4.0 nm particles ($J_1$) were calculated from PSM data at CSIC and ISCIII stations. $GR_{PSM}$ were calculated from 11 to 18 July 2016, averaging 4.3 nm $h^{-1}$ at the urban station and 3.7 nm $h^{-1}$ at the suburban station. $J_1$ were calculated only for the days in which NPF is identified. The results for these days are included in Table 1. Average $J_1$*

*values are higher at the urban station (8.9 $cm^{-3}$ $s^{-1}$) compared to the suburban station (5.3 $cm^{-3}$ $s^{-1}$). Concentrations of 1.2-4.0 nm particles are lower at the urban station (Figure S6), which could lead to lower formation rates. However, the coagulation sink is greater at the urban station, as discussed before, which contributes to the second factor in Eq. (4). It has to be noted that only 3 days of PSM data were available for NPF events at the urban station. A longer dataset could lead to different results.*

*The average values of the formation rates agree with those reported at similar stations around the world. For instance, Woo et al. (2001) reported $J_3$ ranging 10-15 $cm^{-3}$ $s^{-1}$ in Atlanta, US. Wehner and Wiedensohler (2003) reported average $J_3$ of 13 $cm^{-3}$ $s^{-1}$ in Leipzig, Germany. Hussein et al. (2008) reported nucleation rates ($D_p$<25 nm) ranging 2.1-3.0 $cm^{-3}$ $s^{-1}$ in summer in Helsinki.*

5.) **I do not follow the conclusion written in the abstract on lines 37-39: "The vertical soundings demonstrated that ultrafine particles (UFP) are transported from surface levels to higher levels, thus newly formed particles ascend from surface to the top of the mixing layer", or that the fluxes are "bottom-up" as written on page 9, line 28. As far as I can tell, Fig. 10 (which is a very nice figure by the way) only shows that the particles are produced inside the mixed layer (not the residual layer). The mixed layer of course grows during the day, but how can you tell whether the particles are being produced close to the surface or at the top of the mixed layer (or both)?**

We agree with this statement. It was not clear enough. We can only say that the particles are produced inside the mixed layer, which grows during the day. We cannot tell if these particles are produced in a specific altitude inside this layer. This has been clarified in the text.

*The vertical soundings demonstrated that ultrafine particles (UFP) are formed exclusively inside the mixed layer. As convection becomes more effective and the mixed layer grows, UFP particles are detected at higher levels.*

6.) **Regarding shrinkage in lines 1-2 on page 7: Could evaporation be a reason for the shrinkage as well?**

Yes, in fact this is the case. Upon closer inspection of the wind speed and wind direction time series, we determined that wind speed increased during the shrinking phase, but the wind direction did not change substantially, therefore there is no change of air masses and the leading process is dilution, which favors evaporation. The text has been modified as follows:

*The start of the shrinking phase coincides with a marked increase in wind speed, therefore it is associated with dilution, which favors the evaporation of semi-volatile vapors, resulting in a decline in particle diameter and concentrations, as observed in most cases (see Figure 1).*

7.) **Page 7, lines 30-31: "For these stations the observed median growth rates were 7-8 nm h-1". These values are very close to the average growth rate of 7.3 nm h-1 reported from Bakersfield, a polluted location in California (Ahlm et al., 2012). Please also add this reference to the studies of NPF events in urban environments in lines 25-30 on page 2.**

This reference has been added.

**8.) Page 9, line 8. It seems this is the first time you discuss Fig. 3 so perhaps you should change the order of the figures.**

The order of the figures has been modified and this has been corrected.

**9.) I suppose the black dots in Figs. 7-9 represent the fitted log-normal modes, but please add that information to the figure captions.**

Yes. This has been added in the corresponding figure captions (now Figs. 4-6).

*Figure 7: Particle size distribution with fitted log-normal modes (black dots) measured during the balloons soundings at Majadahonda on 12 July 2016.*

**10.) You don't draw any conclusions from Fig. 9 so perhaps that figure is not necessary.**

We think that Fig. 9 (now Fig. 6) gives an additional confirmation of the fact that the particle formation takes place exclusively inside the mixed layer. The figure has been modified following Referee 2 suggestions to include an estimation of the mixed layer height, which adds significance to the figure. We also believe it makes it easier to understand Fig. 10 and we would prefer to keep it.

## References

Ahlm, L., Liu, S., Day, D. A., Russell, L. M., Weber, R., Gentner, D. R., Goldstein, A. H., DiGangi, J. P., Henry, S. B., Keutsch, F. N., VandenBoer, T. C., Markovic, M. Z., Murphy, J. G., Ren, X., and Scott, S.: Formation and growth of ultrafine particles from secondary sources in Bakersfield, California, J. Geophys. Res. Atmos., 117, D00V08, doi:10.1029/2011JD017144, 2012.

Dall'Osto, M., Querol, X., Alastuey, A., O'Dowd, C., Harrison, R.M., Wenger, J., Gómez-Moreno, F.J.: On the spatial distribution and evolution of ultrafine particles in Barcelona. Atmos. Chem. Phys. 13, 741-759, 2013.

Kittelson, D.B., Watts, W.F., Johnson, J.P.: On-road and laboratory evaluation of combustion aerosols – Part1: Summary of diesel engine results. J. Aerosol Sci. 37, 913- 930, 2006.

**REPLY TO #2 REFEREE'S QUERIES AND DESCRIPTION OF CHANGES DONE FOLLOWING HER/HIS SUGGESTIONS**

Many thanks for your valuable comments and suggestions than helped us to improve the quality of the manuscript. As you will see we took into account all your comments when reviewing the new version.

## Major comments

- **Despite the interesting dataset this paper fails in conveying a clear message due to its structure and the way the results are presented. In particular the authors mix the main results (horizontal and vertical characterization of NPF in Madrid) with episodes (e.g. the UFP peaks at night) and phenomena (e.g. shrinkage of particle size) that are not strictly related with them. To address this issue I suggest to the authors to focus more on the important results and emphasize them in a clearer way as well as to restructure the results section in order to make a clear separation between these results and all the minor observations.**

Thanks a lot for your comments. This suggestion has been taken into account and section 3 has been reorganized as follows:

3.1 Meteorological context
3.2 Comparison of NPF events at urban and suburban stations
    3.2.1 Episode characteristics
    3.2.2 Comparison of GR, $J_1$, CS and $CoagS_9$
3.3 Vertical distribution of NPF events
    3.3.1 UFP concentrations
    3.3.2 Particle size distribution
3.4 Other observations
    3.4.1 Prevalence of particles and shrinking
    3.4.2 Nocturnal UFP peaks

- **The authors state several times that NPF is dominating the total particle concentration in Madrid, however it is not clear how they separate between newly formed particles and ultrafine particles directly emitted from cars. I assume that the formation rate calculation is biased by the fact that primary UFP were not taken into consideration and this would explain why formation rates at the urban stations are higher than those measured in the suburban whereas the growth rates are smaller. The authors need to quantitatively estimate the source of UFP and revise the formation rates excluding primary UFP from their results. Doing this would also allow to compare directly the Madrid case with the other locations reported in the introduction. Probably the simplest way to discriminate between primary and secondary UFP would be to use the data of the particle concentrations below 9 nm, that should be available at all the measurement sites.**

Thanks again for this comment. If both referees commented on this, it is because it was not clear enough. We have followed both referees' suggestions to address this issue and we have calculated formation rates using PSM data (see replies to following comments). We have also clarified in the text that we consider NPF events days in which the particle size distributions at all our stations have the same evolution. Being these stations 17 km apart and being all of them of different categories (urban, urban background and suburban), we assume that the particles are not formed in the tailpipe,

i.e., they are not primary. Otherwise there would be significant differences when comparing the PSD at the suburban station, which is not highly influenced by traffic, as opposed to the urban station. Another argument is the fact that particle concentrations measured with the PSM are higher in the suburban station, compared with the urban station (as shown in Fig S7). Additionally, PSM data show an increment in the concentration of all size ranges around the same time in which we begin to see growth in the SMPS size distributions, meaning that these particles started growing from 1.2 nm, therefore they are not 6-11 nm emissions as suggested. Dall'Osto et al. (2013) characterized at regional scale (40 km) the simultaneous occurrence of these photochemical nucleation events covering vast zones with very high nucleation. The following text was modified to clarify this:

*In the selected episodes, intensive daytime nucleation and subsequent condensational growth processes took place simultaneously at urban and suburban stations, located 17 km apart, and accordingly we classify these as regional NPF episodes. Being all stations differently influenced by traffic (influenced, slightly and not influenced by traffic), we can affirm that these episodes are regional events and not representative of primary emissions. Otherwise, we would observe significant differences at our stations. Additional arguments are the fact that number concentrations of sub-25 nm particles peak at noon, when BC levels are at their minimum, as well as higher concentration of particles measured by PSM at the suburban station, compared to the urban station, implying that the particles are not originated from traffic sources.*

- **In section 2.2 no details are provided about the sampling conditions. The authors should give a short description of the inlets and explain for example if losses were measured and/or calculated, if any intercomparison between the different particle counters was performed, etc... Moreover, a big part of the work is based on the measurements performed with the Hy-SMPS but no proper characterization is provided (Figure S2 is not really useful to evaluate the performances of this instrument) and the only cited paper is written in Korean (I'm also not sure whether this is a peer reviewed journal or not). For these reasons a more complete characterization of this instrument is required, for example it could be useful to compare the Hy-SMPS with a reference SMPS while looking at separate size bins and not only at the total concentration.**

TSI instruments were corrected for diffusion losses and multiple charge losses using the instruments' own software. The measuring conditions were the same at all sites. PSM data was post-processed using tailored software provided by Airmodus.

The journal *Particle and Aerosol Research* is published by the Korean Association for Particle and Aerosol Research (KAPAR). It is a peer reviewed journal. A comparison between Hy-SMPS and a TSI SMPS is provided in the supplementary material. Figure S2 has been modified and the following text has been modified in page 2 line 38:

*The instrument was intercompared with a TSI-SMPS (Standard DMA with 3776 CPC) for 50-nm monodisperse NaCl particles and polydisperse aerosol (Fig. S2).*

- **In section 2.3 it is explained how formation and growth rates are calculated, however no explanation is provided about the decision of using the 9-25 nm range, despite the fact that measurements of particle concentrations down to about 1nm were performed. I would argue that this is not the best choice, in particular for the formation rates that could be highly biased by primary emissions as previously explained. Moreover, using a**

**smaller reference diameter for the formation rate would permit to better compare with measurements performed in other locations and/or in chamber studies. For these reasons I would suggest to calculate formation rates for a more meaningful size (below 5 nm) and eventually to calculate growth rates at two different sizes (for example keep the 9-25 nm range for comparability with the vertical sounding and add a lower size GR depending on the availability of the existing data). Finally, uncertainties for all the growth and formation rates should be estimated in order to make a proper comparison between different locations and days.**

We chose this size interval (9-25 nm) due to the detection limit of the SMPS, which is the instrument we used to calculate growth rates, sinks and formation rates. PSM data was very noisy and we preferred not to use it for this purpose. However, following both Referees' comments, the calculations have been made again using PSM data. Figure 6 and previous results using SMPS have been removed. Calculated growth rates and formation rates with PSM have been added to the discussion:

*Growth rates ($GR_{PSM}$) and total formation rates of 1.2-4.0 nm particles ($J_1$) were calculated from PSM data at CSIC and ISCIII stations. $GR_{PSM}$ were calculated from 11 to 18 July 2016, averaging 4.3 nm $h^{-1}$ at the urban station and 3.7 nm $h^{-1}$ at the suburban station. $J_1$ were calculated only for the days in which NPF is identified. The results for these days are included in Table 1. Average $J_1$ values are higher at the urban station (8.9 $cm^{-3}$ $s^{-1}$) compared to the suburban station (5.3 $cm^{-3}$ $s^{-1}$). Concentrations of 1.2-4.0 nm particles are lower at the urban station (Figure S6), which could lead to lower formation rates. However, the coagulation sink is greater at the urban station, as discussed before, which contributes to the second factor in Eq. (4). It has to be noted that only 3 days of PSM data were available for NPF events at the urban station. A longer dataset could lead to different results.*

*The average values of the formation rates agree with those reported at similar stations around the world. For instance, Woo et al. (2001) reported $J_3$ ranging 10-15 $cm^{-3}$ $s^{-1}$ in Atlanta, US. Wehner and Wiedensohler (2003) reported average $J_3$ of 13 $cm^{-3}$ $s^{-1}$ in Leipzig, Germany. Hussein et al. (2008) reported nucleation rates ($D_p$<25 nm) ranging 2.1-3.0 $cm^{-3}$ $s^{-1}$ in summer in Helsinki.*

- **Section 3.2.2 reports a comparison of growth rates and formation rates at the different sites but without including the vertical profiles (in this case growth rates are provided in section 3.3). I think that the paper would benefit by having all the growth rates presented together, this would improve the readability and the clarity of the paper.**

All growth rates, including those of the vertical soundings, were already provided in Table 1, in section 3.2. However, following your suggestion, we have added this information in the discussion of the surface stations to improve the clarity.

*Figure 2 shows the growth rates presented in Table 1 according to urban and suburban surface stations. GR regarding the vertical measurements are provided in the following section due to differing sampling periods.*

- **Section 3.2.3 reports PTR measurements of 3 ions that show some correlation with the particle growth, however this section is not adding any valuable information to the overall picture of the paper. For this reason I would suggest to either remove it or expand it with more detailed analysis. For example it would be worth investigating the possible**

**precursors for HOMs formation. It may be possible to say something about the origin of the condensable vapours by looking at the concentration and diurnal profiles of biogenic vs. anthropogenic VOCs.**

We conceived section 3.2.3 as a brief presentation of interesting preliminary results rather than a central part of the paper. We think that expanding this section is not reasonable, considering both the amount of work needed, and the fact that it is not an essential part of this paper. However, we believe it is worth it to move these results to the supplementary information.

- **Section 3.2.4 should be written in a more consistent way, in particular the authors first speak of sub-25 nm particles but then they only show bivariate plots of sub-4nm particle concentration, what is the reason for this? Moreover to better support the airport hypothesis it would be useful to show a time series of UFP for the period of interest together with wind speed and wind direction (extrapolating these data from the supplementary is difficult due to the long time period reported there). I'm asking this because the bivariate plots only show that UFP particle concentration is higher when the wind is coming from NE but to support the authors hypothesis it would be important to check if there are periods with low UFP concentration under the same wind conditions. If this is the case then I wound find the hypothesis less convincing due to the fact that the airport should be a more or less stationary source of UFP.**

We considered that it was interesting to see if these particles were growing from smaller diameters to better determine their origin, hence the choice to use sub-4nm particle concentration instead of sub-25nm. This has been clarified in the text. We followed your suggestion to better support our hypothesis, and we have included an additional figure in the SI showing PSM data together with wind direction and wind speed, highlighting periods with NE direction and high wind speed, as well as periods with low particle concentration. A version of this figure is presented in Figure D1. The episodes described in the manuscript (12-14 July) coincide with NE directions and high wind speed. During the sampling period, there are not other periods in which these two conditions apply simultaneously. Therefore, according to the available data, there are no periods with low UFP under the same wind conditions. The following text has been added to the discussion in the corresponding section:

*To better support this hypothesis, Fig. S7 shows PSM data together with wind direction and wind speed, showing that the episodes coincide with strong NE winds, and that there are not episodes with low UFP concentrations with these same conditions.*

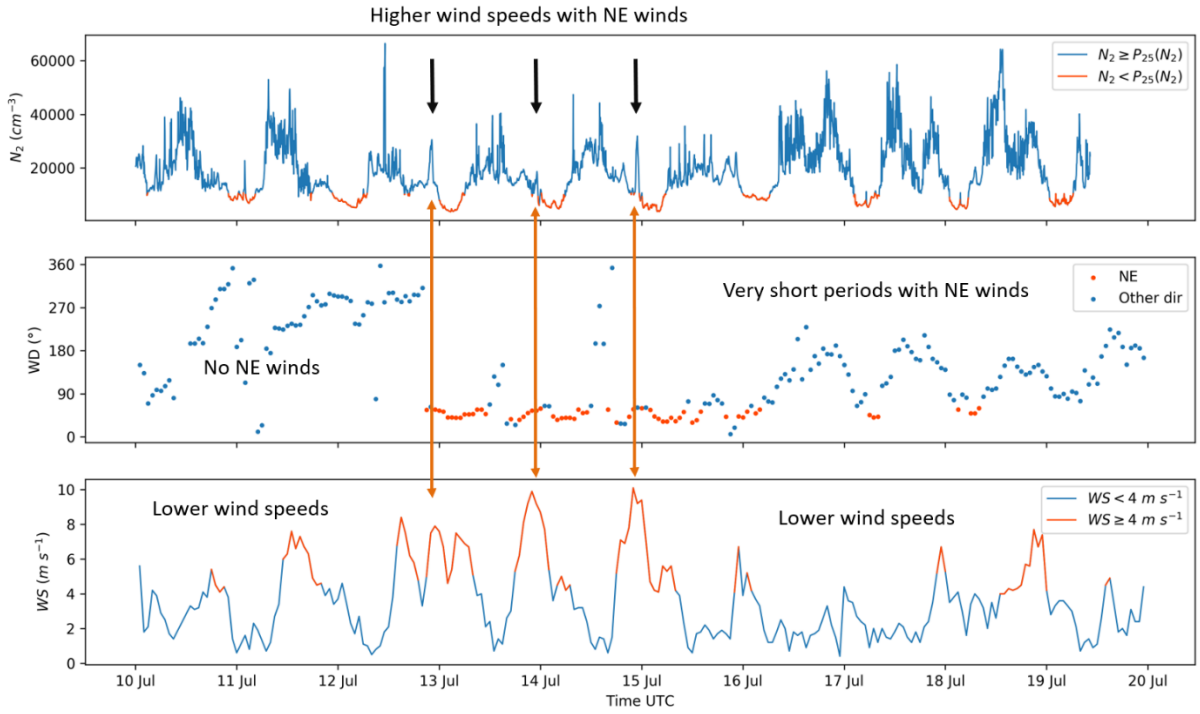


Figure D1: Concentration of particles >2 nm measured with PSM at CSIC station, wind direction and wind speed from 10 to 20 July 2016. $N_2$ lower than 25$^{th}$ percentile has been highlighted, as well as NE directions and wind speeds higher than 4 m/s.

- **In section 3.3 the authors often speak of "bottom-up flux" for the UFP however, what vertical profiles show is only that the UFP concentration is homogeneous inside the mixing layer. For this reason one should avoid using this terminology and the authors should correct all the corresponding parts in the paper. Moreover, I found that the interpretation of the vertical profiles graphs is complicated by the absence of a direct measurement of the mixing layer height. Referring to the "twin paper" [1], this information should be available for all the soundings (for example the potential temperature or total particle concentration can be used) and it would be a really nice addition to the graphs.**

We agree with this statement. We can only say that the particles are produced inside the mixed layer, which grows during the day. We cannot tell if these particles are produced in a specific altitude inside this layer. This has been clarified in the text.

A rough estimation of the mixing layer height has been added to the plots as suggested. The following text has been added in sections 2 and 3:

*Particle concentration in the range 3-1000 nm was measured with a miniaturized butanol-based CPC (Hy-CPC). The time resolution was 1 s, and sample flow was 0.125 L/min (Lee et al., 2014).*

*A rough estimation of the mixed layer height was determined using Hy-CPC measurements. The top of the mixed layer was considered at an altitude in which particle concentration decreases an order of magnitude quasi-instantaneously and remains constant above. All UFP profiles are included in Querol et al. (2018).*

*The interphase between the mixed layer and the residual layer, i.e. the mixed layer height, has been derived using the UFP vertical profiles (see Querol et al., 2018).*

- **The conclusions are written as a summary of the paper but here the author should focus more on the significance of their findings compared with existing observations. This section should be rewritten in order to convey a clearer message, so I suggest to the authors to delete all the unnecessary parts focusing more on the important results of the paper.**

Following your directions, we have re-written the conclusions as follows:

*We investigated the phenomenology of regional and secondary New Particle Formation (NPF) episodes in central Spain. To this end we set up 3 supersites (an urban, a urban background and a sub-urban background) 17 km away in and around Madrid. We were able to characterize 6 NPF events, and in all cases the evolution of the particle size distribution (PSD) was very similar at all stations: around sunrise nucleation mode particles appear and start growing and in the afternoon a decline in particle sizes, i.e. shrinkage, is observed. The regional origin of the NPF is supported by the simultaneous variation in PSD in the nucleation mode and particle number concentrations, growth and shrinkage rates. Furthermore, time trends of condensation and coagulation sinks (CS and CoagS) were similar at all stations, having minimum values shortly before sunrise and increasing after dawn towards the maximum value after midday in the early afternoon. In spite of the 17 km scale simultaneous processes affecting particle number concentrations, the following relevant differences between urban and suburban stations were observed: i) the urban stations presented larger formation rates and smaller growth rates as compared to the suburban stations; ii)in general, the sinks were higher at the urban stations.*

*Regarding the vertical soundings of the NPF events, we observed that in the early morning the vertical distribution of newly formed particles is differentiated in two layers. The lower layer (mixed layer, ML) in which convection is effective, is well-mixed and has a homogeneous PSD. This ML heightens throughout the day, as insolation is more pronounced, extending beyond the sounding limits around midday. NPF occurs throughout this ML, and growth rates and concentrations are homogeneous. The upper layer is a stable residual one (RL) in which particles formed or transported the previous days prevail. In the RL growth is inhibited or even completely restrained, compared with the same particles in the ML. Overall, the soundings demonstrate that particles are formed inside the ML, but they can prevail and be displaced and stored at upper levels and continue to evolve on following days.*

*Additionally, a few nocturnal bursts of nucleation mode particles were observed in the urban stations, which could preliminarily be related with aircraft emissions transported from the airport of Madrid.*

*In this campaign we could not measure in the earliest stages of NPF due to safety requirements of the balloon flights early in the morning. We think it is important for future work to carry out soundings during the nucleation phase of the episodes. However, miniaturized instruments able to measure smaller particles would be needed, which are not available at the present time. This would allow us to determine whether secondary NPF takes place throughout the ML or occurs at the surface and is transported upwards by convection afterwards. If the former were true, then locations with high ML could produce more secondary particles than we have considered, and they could affect a larger population, or influence climate to a greater extent.*

*We cannot determine whether the NPF episodes were triggered by the pollution generated in the city that extended to the region, or the events are caused by a broader phenomenon. In either way, it can be concluded that in summer the particle number concentrations are dominated by NPF in a wide area. The impact of traffic emissions on concentrations of UFP is much smaller than those of NPF, even near the city center where the pollution load is at the highest. This result is in line with other studies performed in cities from high insolation regions (e.g. Kulmala et al., 2016). Given the extent of the episodes, the health effects of NPF can affect a vast number of people, considering that the Madrid metropolitan area with more than 6 million inhabitants is the most populated area in Spain, and one of the most populated in Europe (UN, 2008). For this reason, we believe that the study of health effects related to newly-formed particle inhalation is crucial.*

## Minor comments

- **Page2 line 3: "The NPF events extend over the full vertical extension of the mixed layer reaching as high as 3000 m." But the maximum height of the sounding is 2000 m, so this should be corrected.**

Although the maximum height of the sounding is 2000 m, we state that the events take place over the full extension of the mixing layer, which other authors (e.g. Plaza et al., 1997) have found to reach as high as 3000 m. This sentence has been rewritten to clarify this.

*The NPF events extend over the full vertical extension of the mixed layer, which can reach as high as 3000 m in the area, according to previous studies.*

- **Page 2 line 4: "This can have consequences in the radiative balance of the atmosphere and affect the climate", the climatological effect of NPF in a polluted environment as Madrid is questionable and not supported by any evidence in this paper, for this reason remove or rephrase this sentence.**

We agree with this comment. Since we do not provide any evidence for this we have removed this sentence.

- **Page 2 line 5: As previously stated, a proper estimation of NPF over primary UFP should be given here.**

See reply to the second major comment.

- **Page 2 line 25: There is no need to cite 25 papers, this can be reduced.**

We have reduced the number of citations.

- **Page 3 line 13: The sentence seems to contradict the cited paper of Querol et al.[1] where it is said that "Relatively low concentrations of ultrafine particles (UFPs) were found during the study, and nucleation episodes were only detected in the boundary layer."**

On page 3 lines 13-15 it is said that "intensive NPF episodes take place inside the planetary boundary layer (PBL) in Barcelona, occurring around midday at surface levels when insolation and dilution of pollution are at their maxima". This agrees with the statement quoted from [1].

- **Page 4 line 13: It would be useful to add a scale to the map in figure S1.**

Figure S1 has been modified accordingly.

- **Page 4 line 19: It is not clear if the PSM was operated in scanning mode or fixed mode, it would be good to specify this.**

The PSM was operated in scanning mode. This has been specified in the text.

*[…] and a Particle Size Magnifier (PSM) (AirModus) in scanning mode for the size range 1.2-2.5 nm.*

- **Page 6 line 14: It is said that NPF was identified on 12 days but table 1 only reports 7 days so this should be made consistent. Moreover, Figure S8 shows that there were 2 nucleation events at CIEMAT on the 13th and 14th of July that are not mentioned in the table. In addition, it would be useful to add also formation rates to the table together with the GR values.**

This is a mistake, we wanted to say that we selected 12 episodes amongst the 18 the identified episodes, considering all stations, occurring on 6 days (7 days identified). We have rewritten this sentence to make it clear:

*18 NPF episodes have been identified on a total of 7 days throughout the campaign. In Table 1 a summary of these events is presented. Out of these, a total of 14 events on 6 days had simultaneous data available for at least one of the urban stations (CSIC, CIEMAT) and the suburban station (ISCIII).*

We have added formation rates $J_1$ to the table as suggested.

- **Page 6 line 27: It's almost impossible to see the early morning UFP concentration just by looking at the full time series. Thus a dedicated plot should be made either by plotting sub-10nm particles on top of Figure 1 or by plotting a diurnal profile for this size range.**

Figure 5 (now Fig. 3) has been modified to include a diurnal profile of total particle concentration using PSM data, as suggested in other comments.

- **Page 7 line 1: Particle size shrinking is an interesting phenomenon but it doesn't fit nicely in this part of the text. For this reason describe it in a separate (small) section. It would also be nice to plot the wind speed specifically for the shrinking phase because from the overall plot it is difficult to see a trend. In some cases also a rapid change in number concentrations is observed pointing to a change in air mass. In these cases it does not make sense to speak about a shrinking of aerosols because the aerosol population changes. The authors should demonstrate clearly, that the same population of aerosols is shrinking. Otherwise, it is not shrinking and they should delete this.**

We agree with this comment. Following your suggestions, we have moved the shrinking discussion to a short section.

Upon closer inspection of daily plots of wind speed and wind direction (Fig. S7), we determined that wind speed increased during the shrinking phase, but the wind direction did not change substantially, therefore there is no change of air masses and the leading process is dilution, which favors evaporation. The text has been modified as follows:

*The start of the shrinking phase coincides with a marked increase in wind speed, therefore it is associated with dilution, which favors the evaporation of semi-volatile vapors, resulting in a decline in particle diameter and concentrations, as observed in most cases (see Figure S7).*

This new figure has been added to the supplementary information (Fig. S7).

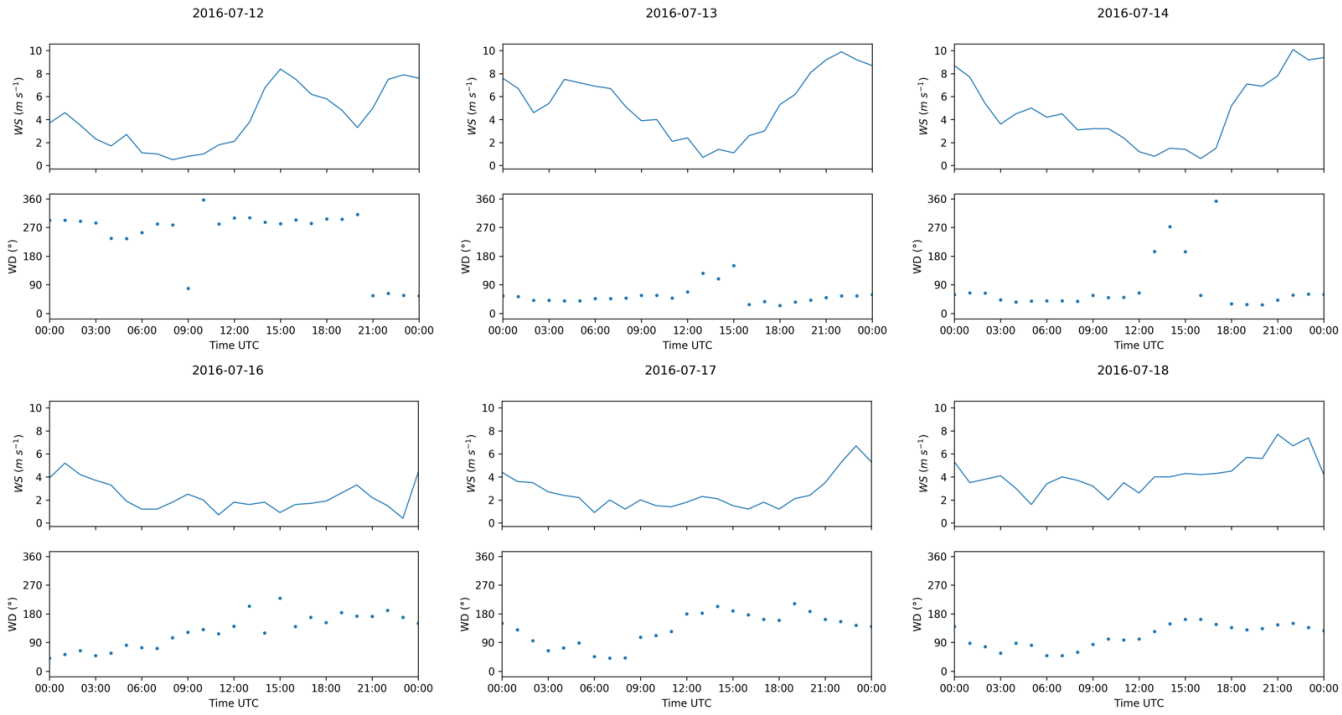


Figure S7: Daily plots of wind speed and wind direction for the days in which shrinkage is observed.

- **Page 7 line 14: Here a reference to Figure 5 would be useful. Moreover, I think that associating UFP with particles in the range 9-25 nm is misleading and it would be better to plot the diurnal profile for all particles below 25 nm and for the total particle concentration.**

Following the first comment we have restructured the text and this is not an issue any more.
As mentioned in the previous comment, daily averages of total particle concentration using PSM data have been added to Fig. 5.

- **Page 8 line 5: "above" should be replaced by "below".**

This has been replaced by a reference to the section in which the results are discussed.

- **Page 8 line 11: "The fact that J9 is higher at the urban stations is probably linked to higher traffic emissions [...] in the city, and not related with higher nucleation rates, since PSM measurements indicate lower concentrations of 1.2-4 nm particles". Here the authors confirm my hypothesis that primary particles affect formation rates, underlining the necessity to take this process into account in their calculation.**

As mentioned above, formation rates have been calculated again using PSM data to evaluate this fact and the corresponding results have been added to the discussion.

- **Page 8 line 14: This is not figure S4 but figure S7.**

The order of the figures has been revised and this has been corrected.

- **Page 8 line 14: "The calculated formation rates agree with those reported in other studies, ranging 0.01-10 cm-3s-1 during regional events around the world." I don't see any reason for reporting an agreement within 4 orders of magnitudes. The formation rates measured during this campaign should be compared in a more targeted way with other locations around the world.**

Once formation rates have been calculated with PSM data this has been revised as follows:

*With average values of 8.9 and 5.3 $cm^{-3}$ $s^{-1}$ at the urban and suburban station respectively, the calculated formation rates agree with those reported at similar stations around the world. For instance, Woo et al. (2001) reported $J_3$ ranging 10-15 $cm^{-3}$ $s^{-1}$ in Atlanta, US. Wehner and Wiedensohler (2003) reported average $J_3$ of 13 $cm^{-3}$ $s^{-1}$ in Leipzig, Germany. Hussein et al. (2008) reported nucleation rates ($D_p$<25 nm) ranging 2.1-3.0 $cm^{-3}$ $s^{-1}$ in summer in Helsinki.*

- **Page 8 line 30: "Thus, the particles growth appears to be driven by the uptake of secondary organic compounds." This is a reasonable assumption but cannot be proven by the PTR measurements presented in this work. Try to support this assumption with additional information, for example one can try to check if the growth rates can be explained by sulfuric acid alone (assuming a reasonable range of values for sulfuric acid concentration) or not.[2, 3]**

We don't have the data needed to support this assumption. We have stated in the text that $SO_2$ levels were below the detection limit of the standard air quality UV spectrometry instruments during all the period. This has been added to the text, which has been moved to the SI as stated in a previous comment.

*We cannot prove this assumption using the PTR-ToF-MS measurements. We cannot check if the growth rates can be explained by sulfuric acid alone, since $SO_2$ levels were below the detection limit of the standard air quality UV spectrometry instruments during all the period.*

- **Page 10 line 10: "the mode slightly decreases its size when the sounding ascends above the mixed layer limit", as already written above the mixing layer height should be plotted together with the particle size distribution to better visualize these changes.**

An estimation of the mixed layer height has been provided in the corresponding figures.

- **Page 10 line 12: It would be good if the authors could specify how they calculated the growth rate in the residual layer. The impressions from the graphs is that there are really few points inside the residual layer and it is not clear whether there is any growth at all inside this layer.**

The growth rate here was calculated in the same way that in the mixed layer, selecting only the points inside the residual layer. Even though it might be not clear in the graphs, there are enough points to carry out the calculations when zooming in into the short time period of interest. In the presented graphs the dots are overprinted and it might look like there are not enough points to carry out these calculations.

- **Page 10 line 15: I'm not really convinced by the presence of a 10 nm mode in the first sounding, Maybe there is an over-fitting issue with the mode fitting algorithm. For this reason I think calculation of the growth rate is questionable and should be avoided.**

We believe that this is not an over-fitting. The same mode is observed simultaneously at the nearby (<3 km) ISCIII station at surface level using TSI instruments. We added this to the text to justify the calculation.

*Moreover, during the morning we observed particles growing inside the mixing layer from 10 nm at 7:00 UTC, to 30 nm at midday, with a growth rate of 3.5 nm $h^{-1}$. This mode is observed simultaneously at ISCIII and therefore we consider it for calculation. The growth rate obtained is 3.5 nm $h^{-1}$.*

- **Page 10 line 23: "The accumulation mode grows from 156 nm at 07:00 UTC to 200 nm at 10:00 UTC", also in this case I think the accumulation mode is over-fitted, the authors should either revise their fitting algorithm or prove that I'm wrong by reporting in the SI a single SMPS scan plot with the fitted modes on top of it.**

We agree, we removed all the results regarding the accumulation mode because we cannot prove that the fitting is correct for the accumulation mode.

- **Page 10 line 26: "Another mode starting roughly at 40 nm at 09:00 UTC" I guess this should be 07:00 UTC.**

Yes, this has been corrected.

- **Page 10 line 30: I don't see any nucleation mode earlier than 09:30-10.00 UTC. Correct this sentence and eventually revise the calculated growth rate.**

The fitting algorithm considers the appearance of the nucleation mode by 8:00 UTC, but we agree that we can't consider it until at least 9:00 UTC. Comparing with other stations, we considered that the mode appears at 9:00 UTC and calculated all growth rates from that time. The sentence has been rewritten to clarify this.

*A nucleation mode grows from the detection limit of the instrument, around 10 nm at 08:30 UTC to 40 nm at 15:00 UTC. Comparing with other stations, we considered this mode only after 9:00 UTC, and calculated the growth rates from that time. We consider this a regional NPF event, since the start of the particle growth is registered simultaneously at all the stations. The growth rates at the sounding location, ISCIII and CSIC are 5.3 nm $h^{-1}$, 4.6 nm $h^{-1}$ and 2.0 nm $h^{-1}$, respectively.*

- **Page 10 line 38: "As the insolation increased, so did the altitude of the mixing layer, until it reached the altitude at which the balloons were positioned." By looking at the plot it seems more likely that the balloon height decreased until reaching the mixing layer.**

The tethered balloons were positioned at a fixed altitude, meaning that the extension of the wire was not modified during these flights. However, wind conditions can vary the altitude of the instruments – for example increasing or decreasing horizontal wind speed – and this is what we see from 9:30 to 10:30 UTC in Fig. 9 (now Fig. 6). We have modified the text to explain this.

*In order to verify this result two constant altitude flights were made during the morning. The extension of the wire was not modified during these flights. However, changing wind conditions varied slightly the altitude of the instruments. The altitude was chosen so that the instruments remained initially outside the mixing layer, i.e. inside the residual layer.*

- **Page 10 line 40: As previously explained avoid speaking of particles flowing upward, measurements are just showing that UFP are homogeneous inside the mixed layer.**

This has been corrected accordingly as follows:

*As the mixing layer reached the balloons, total particle concentration sharply increased from $4x10^3$ to $2x10^4$ $cm^{-3}$, demonstrating that newly-formed particles remain inside the mixing layer.*

- **Page 11 line 5: I do not see a growth of 40 nm particles in the residual layer. The size of this mode is the same at the 9 and 11 UTC sounding.**

There is growth of this mode, revealed by the growth rate calculation. This might not be evident visually due to the use of a log-scale. However, the text has been clarified to make it clearer.

*Inside the residual layer particles had a slower growth rate (0.5 nm $h^{-1}$ compared to 8.45 nm $h^{-1}$ for the 40 nm mode – note that due to the use of a log-scale this might be unnoticeable visually), and no particles smaller than 20 nm were observed.*

- **Page 11 line 6: how do you know that you observed these particles already the previous day? Moreover, also here I think that the Aitken mode is over-fitted.**

There is a mistake in this sentence. We were referring to the accumulation mode. Following other comments, we removed all results regarding accumulation-mode particles and this sentence has been removed.

However, this comment applies to the discussion of Fig. 7. We know that they are the same particles by definition of the residual layer:
About a half hour before sunset the thermals cease to form, allowing turbulence decay in the formerly well-mixed layer. The resulting layer of air is called residual layer because its initial mean state variables and concentration variables are the same as those of the recently-decayed mixed layer. […] The residual layer often exists for a while in the mornings before being entrained into the new mixing layer. [4]
Since an approximation of the mixing layer height has been provided following the suggestions of previous comments, we can affirm that this layer is above the mixing layer, and therefore it is the residual layer, which contains the particles that were observed in the mixed layer the day before. This has been stated in the text when discussing Fig. 7, and a reference was added.

*The fact that sub-40 nm particles are not detected at the higher levels of the first flights suggests that convection is not very effective yet, and the sounding goes through different atmospheric layers, most likely the mixed layer and the residual layer. In the residual layer Aitken-mode particles formed on previous days prevail (Stull, 1988).*

- **Page 11 line 16 and following lines: I would avoid speaking of the accumulation mode. I'm really sceptical about the presence of this mode in the measurements presented here and, even if it is present, then it is above the detection limit for most of the time. Moreover, it is said that the accumulation mode grew faster than the other modes and "this phenomenon has been rarely reported in ambient air." I think the data do not support this conclusion. If I'm not mistaken the fitted accumulation mode shows a growth only for a couple of hours on a specific day and the data are quite scattered so it doesn't**

**seem like the growth is significantly higher compared with the Aitken mode. If the authors want to support this observation then they should try to look if anything similar is present in the SMPS ground measurements.**

As mentioned in a previous comment, we have removed all the results involving the accumulation mode, since we cannot prove that this mode is not over-fitted.

- **Page 12 line 13,14: As already explained the vertical profiles do not show a clear accumulation mode and this is particularly true for the residual layer, so I would remove this sentence.**

See previous comment.

- **Page 12 line 18: the authors don't need a miniaturized instrument with "greater resolution" but an instrument able to measure smaller particles.**

We agree with this comment and it has been corrected in the text.

*However, miniaturized instruments able to measure smaller particles would be needed, which are not available at the present time.*

- **Figure 1: I would greatly recommend to avoid using jet colormap (i.e. rainbow colormap) for surface plots. This colormap is not perceptually uniform and this can create several kinds of issues as widely documented elsewhere (e.g. https://www.ncbi.nlm.nih.gov/pubmed/22034369 and http://ieeexplore.ieee.org/document/4118486/?reload=true)**

This figure has been replaced by the former Figure S8, because the latter contains the same information in a clearer presentation, in addition to information regarding total particle concentration, as suggested in another comment. However, a rainbow colormap is also used in the new figure because of the limitations of the software used to produce the plot (Igor Pro, WaveMetrics).
Following this suggestion, we have changed the colormap in previous Figure 10 (now Fig. 7), which was also using jet colormap.

- **In Figure S8 the authors report the total size distribution for the three measurement sites. This is a useful supplementary information but the readability of the graph should be improved. In particular a logarithmic color scale should be used as well as a higher image resolution. I also suggest to extrapolate the total particle number concentration for the 3 sites in the same size bins for better comparability rather than using different sizes for each site. Finally I noticed that there are some mismatches in the merged size distributions measured at CIEMAT (e.g. 8/7/2016). This would indicate that one of the instruments was not working properly. Please comment on this. How would this affect the presented results?**

The figure has been modified, using a logarithmic color scale as suggested, and the total particle number concentration is now used for the 3 sites.
The fact that there is a mismatch in the size distributions at CIEMAT is because the two instruments were measuring in different size ranges. The instrument measuring the smallest particles had more losses. This was corrected prior to the calculations; however, we didn't include the corrections in

this figure. Now the figure has been corrected to take this into account and a description of the corrections made has been added in section 2 as follows.

*Important discrepancies were observed after merging both SMPS particle size distributions. In order to correct that, we studied the distribution of particles in the coinciding size range (14-31 nm). The daily nanoSMPS size distribution was divided by the daily average of this range. We compared the resulting merged particle size distribution with CPC measurements, to check that there was a good agreement in the total particle concentration.*

## References


[1] X. Querol et al. “Phenomenology of summer ozone episodes over the Madrid Metropolitan Area, central Spain". In: Atmospheric Chemistry and Physics Discussions 2017 (2017), pp. 1-38. doi: 10.5194/acp-2017-1014. url: https://www.atmos-chem-phys-discuss.net/acp-2017-1014/ (cit. on pp. 3, 4).

[2] T. Nieminen et al. “Sub-10 nm particle growth by vapor condensation effects of vapor molecule size and particle thermal speed". In: Atmospheric Chemistry and Physics 10.20 (2010), pp. 773-9779. issn: 16807316. doi: 10.5194/acp-10-9773-2010 (cit. on p. 5).

[3] Jasmin Tröstl et al. “The role of low-volatility organic compounds in initial particle growth in the atmosphere". In: Nature 533.7604 (2016), pp. 527-531. issn: 0028-0836. doi: 10.1038/nature18271. url: http://www.nature.com/doifinder/10.1038/nature18271 (cit. on p. 5).

[4] Roland B. Stull. “An introduction to boundary layer meteorology”. Kluwer Academic Publishers, Dordrecht, Boston and London, 1988.

# Vertical and horizontal distribution of regional new particle formation events in Madrid

Cristina Carnerero[1,2], Noemí Pérez[1], Cristina Reche[1], Marina Ealo[1], Gloria Titos[1], Hong-Ku Lee[3], Hee-Ram Eun[3], Yong-Hee Park[3], Lubna Dada[4], Pauli Paasonen[4], Veli-Matti Kerminen[4], Enrique Mantilla[5], Miguel Escudero[6], Francisco J. Gómez-Moreno[7], Elisabeth Alonso-Blanco[7], Esther Coz[7], Alfonso Saiz-Lopez[8], Brice Temime-Roussel[9], Nicolas Marchand[9], David C. S. Beddows[10], Roy M. Harrison[10,11], Tuukka Petäjä[4], Markku Kulmala[4], Kang-Ho Ahn[3], Andrés Alastuey[1], Xavier Querol[1]

[1]Institute of Environmental Assessment and Water Research (IDAEA-CSIC), Barcelona, 08034, Spain.

[2]Department of Civil and Environmental Engineering, Universitat Politècnica de Catalunya, Barcelona, 08034, Spain.

[3]Department of Mechanical Engineering, Hanyang University, Seoul, Republic of Korea.

[4]Department of Physics, University of Helsinki, Helsinki, 00560, Finland.

[5]Centro de Estudios Ambientales del Mediterráneo, CEAM, Paterna, 46980, Spain.

[6]Centro Universitario de la Defensa de Zaragoza, Academia General Militar, Zaragoza, 50090, Spain.

[7]Department of Environment, Joint Research Unit Atmospheric Pollution CIEMAT, Madrid, 28040, Spain.

[8]Department of Atmospheric Chemistry and Climate, Institute of Physical Chemistry Rocasolano (IQFR-CSIC), Madrid, 28006, Spain.

[9]Aix Marseille Univ, CNRS, LCE, Marseille, 13003, France.

[10]National Centre for Atmospheric Science, University of Birmingham, B15 2TT, United Kingdom.

[11]Department of Environmental Sciences, Centre for Excellence in Environmental Studies, King Abdulaziz University, Jeddah, 21589, Saudi Arabia.

*Correspondence to*: Cristina Carnerero (cristina.carnerero@idaea.csic.es)

**Abstract.** The vertical profile of new particle formation (NPF) events was studied by comparing the aerosol size number distributions measured aloft and at surface level in a suburban environment in Madrid, Spain using airborne instruments. The horizontal distribution and regional impact of the NPF events was investigated with data from three urban, urban background and suburban stations in the Madrid metropolitan area. Intensive regional NPF episodes followed by particle growth were simultaneously recorded at three stations in and around Madrid, in a field campaign in July 2016. The urban stations presented larger formation rates and smaller growth rates compared to the suburban station. Condensation and coagulation sinks followed a similar evolution at all stations, with higher values at urban stations. However, total number concentration of particles bigger than 2.5 nm was lower at the urban station and peaked around noon, when BC levels are minimum. ~~On some days a marked decline in particle size (shrinkage) was observed in the afternoon, associated with a change in air masses. Additionally, a few nocturnal nucleation mode bursts were observed in the urban stations, which could be related to aircraft emissions transported from the airport. Considering all simultaneous diurnal NPF events registered, growth rates were significantly lower at the urban stations, ranging 2.0-3.9 nm $h^{-1}$, compared to the suburban station (2.9-10.0 nm $h^{-1}$). Total concentration of 9.1-25 nm particles reached 2.8 x $10^4$ $cm^{-3}$ at the urban station and 1.7 x $10^4$ $cm^{-3}$ at the suburban station, the mean daily values being 3.7 x $10^4$ $cm^{-3}$ (2.2 x $10^4$ $cm^{-3}$ at the suburban station) during event days. The formation rates of 9-25 nm particles peaked around noon and recorded a median value of 2.0 $cm^{-3}$ $s^{-1}$ and 1.1 $cm^{-3}$ $s^{-1}$ at the urban and suburban stations, respectively. The condensation and coagulation sinks presented minimum values shortly before sunrise, increasing after dawn reaching the maximum value at 14:00 UTC, with average daily mean values of 3.4 x $10^{-3}$ $s^{-1}$ (2.5 x $10^{-3}$ $s^{-1}$ at the suburban station) and 2.4 x $10^{-5}$ $s^{-1}$, respectively, during event days.~~ The vertical soundings demonstrated that ultrafine particles (UFP) are ~~transported from surface levels to higher levels, thus newly formed particles ascend from~~

surface to the top of formed exclusively inside the mixeding layer. As convection becomes more effective and the mixed layer grows, UFP particles are detected at higher levels. The morning soundings revealed the presence of a residual layer in the upper levels in which aged particles (nucleated and grown on previous days) prevail. The particles in this layer also grow in size, with growth rates significantly smaller than those inside the mixed layer. Under conditions with strong enough convection, the soundings revealed homogeneous number size distributions and growth rates at all altitudes, which follow the same evolution in the other stations considered in this study. This indicates that NPF occurs quasi-homogenously in an area spanning at least 17 km horizontally. The NPF events extend over the full vertical extension of the mixed layer, which can reaching as high as 3000 m in the area, according to previous studies. On some days a marked decline in particle size (shrinkage) was observed in the afternoon, associated with a change in air masses. Additionally, a few nocturnal nucleation mode bursts were observed in the urban stations, which could be related to aircraft emissions transported from the airport. This can have consequences in the radiative balance of the atmosphere and affect the climate. Results also evidenced that total particle concentration in and around Madrid in summer is dominated by NPF during summer, thus it may obscure the impact of vehicle exhaust emissions on levels of UFP.

## 1 Introduction

In urban areas, traffic emissions are a major source of UFP (Kumar et al., 2014; Ma and Birmili, 2015; Pey et al., 2008; Pey et al., 2009; Dall'Osto et al., 2012; Salma et al., 2014; Paasonen et al., 2016). These emissions include primary UFP exhaust emissions (Shi and Harrison, 1999; Shi et al., 2000; Charron and Harrison, 2003; Uhrner et al., 2012); cooling of engine exhaust emissions and condensation of semi-volatile phases vapor species that creates new UFP during dilution (Charron and Harrison, 2003; Kittelson et al., 2006; Robinson et al., 2007; Rönkkö et al., 2017). These are also considered primary particles, since they are formed near the source. Other relevant UFP sources include industrial emissions (Keuken et al., 2015; El Haddad et al, 2013), city waste incineration (Buonanno and Morawska, 2015), shipping (Kecorius et al, 2016; Johnson et al., 2014), airports (Cheung et al., 2011; Hudda et al., 2014; Keuken et al., 2015) and construction works (Kumar and Morawska, 2014).

New particle formation (NPF) from gaseous precursors has been shown to cause high ultrafine particle (UFP) episodes in relatively clean atmospheres due to low condensation sinks (CS) originating from low pre-existing particle concentration (e.g. Kulmala et al., 2000; Boy and Kulmala, 2002; Wiedensohler et al.,2002; Kulmala et al., 2004; Wehner et al., 2007; O'Dowd et al., 2010; Sellegri et al., 2010; Vakkari et al., 2011; Cusack et al., 2013a; Cusack et al., 2013b; Tröstl et al., 2016; Kontkanen et al., 2017). However, at mountain sites, precursors' availability seems to be the most influential parameter in NPF events, with higher values of CS during NPF events than during non NPF events (Boy et al., 2008; Boulon et al., 2010; García et al., 2014, Nie et al., 2014, among others). Tröstl et al. (2016) reported experimental results on nucleation driven by oxidation of Volatile organic compounds (VOCs), and Kirkby et al. (2016) reported pure biogenic nucleation.

Globally, and especially in urban areas, traffic emissions are a major source of UFP (Kumar et al., 2014; Ma and Birmili, 2015; Pey et al., 2008; Pey et al., 2009; Dall'Osto et al., 2012; Salma et al., 2014; Paasonen et al., 2016) and these arise from primary UFP exhaust emissions (Shi and Harrison, 1999; Shi et al., 2000; Charron and Harrison, 2003; Uhrner et al., 2012), condensation of semi volatile phases vapor species that creates new UFP during dilution and cooling of engine exhaust emissions near the source (Charron and Harrison, 2003; Kittelson et al., 2006; Robinson et al., 2007). Since these are formed very close to the source, most studies consider them as primary (e.g. Brines et al., 2015; Paasonen et al., 2016) or quasi-primary particles (Rönkkö et al., 2017). Other relevant UFP sources include industrial emissions (Keuken et al., 2015; El Haddad et al, 2013), city waste incineration (Buonanno and Morawska, 2015), shipping (Kecorius et al, 2016; Johnson et al., 2014), airports (Cheung et al., 2011; Hudda et al., 2014; Keuken et al., 2015) or even construction works (Kumar and Morawska, 2014).

NPF events contribute also significantly to ambient UFP concentrations in urban environments (~~Woo et al., 2001; Alam et al., 2003; Stanier et al., 2004; Wu et al., 2008;~~ Costabile et al., 2009; ~~Reche et al., 2011; Rimnácová et al., 2011; Salma et al., 2011; Salma et al., 2016; Harrison et al., 2011; Gómez-Moreno et al., 2011.;~~ Wegner et al., 2012; von Bismarck-Osten et al., 2013; ~~Dall'Osto et al., 2013; Betha et al., 2013; Cheung et al., 2011; Hussein et al., 2014; Liu et al., 2014; Salimi et al.,~~ 2014; ~~Brines et al., 2014; Brines et al., 2015;~~ Ma and Birmili, 2015; ~~Minguillón et al., 2015;~~ Hofman et al., 2016, Kontkanen et al., 2017). Common features enhancing urban NPF are high insolation, low relative humidity, availability of $SO_2$ and organic condensable vapors, and low condensation and coagulation sinks (Kulmala et al., 2004; Kulmala and Kerminen, 2008, Sipilä, et al., 2010, Salma et al., 2016). Urban NPF episodes can be either regionally or locally driven and may or may not impact regional background areas (Dall'Osto et al., 2013; Brines et al., 2015; Salma et al., 2016). Cheung et al. (2011) and Brines et al. (2015) reported that in urban areas nucleation bursts without growth of particles are common; whereas the frequently occurring 'banana like' nucleation bursts at regional background sites are scarcely detected at urban sites, probably because the high CS at traffic rush hours limits the duration of the particle growth. These processes seem to prevail in summer and spring in Southern European urban areas (Dall'Osto et al., 2013; Brines et al, 2014; Brines et al., 2015). Brines et al. (2015) also reported that in urban environments the highest $O_3$ levels occur simultaneously with NPF events, as well as the highest $SO_2$ concentrations and insolation, and the lowest relative humidity and NO and $NO_2$ levels. This close association between $O_3$ and UFP may be due to ambient conditions that favor two different but simultaneous processes, or to the fact that they are two products of photochemical reactions in the same overall process.

Reche et al. (2011) evaluated the prevalence of primary versus newly formed UFP in several European cities and found a different daily pattern for the southern European cities, where the newly formed particles contributed substantially to the annual average concentrations, probably because of high insolation and possible site-specific chemical precursors. Brines et al. (2015) determined that NPF events lasting for 2 h or more occurred on 55 % of the days and those extending 4 h on 28 % of the days, being NPF the main contributor on 14-19 % of the time in Mediterranean and Sub-tropical climates (Barcelona, Madrid, Roma, Los Angeles and Brisbane). The latter percentages reached 2 % and 24-28 % in Helsinki and Budapest (Wegner et al., 2012 and Salma et al., 2016, respectively). Furthermore, Brines et al. (2015) calculated that 22 % of the annual average UFP number concentration recorded at an urban background site of Barcelona originated from NPF. Ma and Birmili (2015) reported that the annual contribution of traffic on UFP number concentration was 7, 14 and 30 % at roadside, urban background and rural sites respectively, in and around Leipzig, Germany. On the other hand, traffic emissions contributed 44-69 % to UFP concentrations in Barcelona (Pey et al., 2009; Dall'Osto et al., 2012, Brines et al., 2015), 65 % in London (Harrison et al., 2011; Beddows et al., 2015) and 69 % in Helsinki (Wegner et al., 2012).

Minguillón et al. (2015) and Querol et al. (2017~~a~~) demonstrated that intensive NPF episodes take place inside the planetary boundary layer (PBL) in Barcelona, occurring around midday at surface levels when insolation and dilution of pollution are at their maxima. Earlier in the morning NPF can only take place at upper atmospheric levels, at an altitude where pollutants are diluted, since at surface levels a high CS prevents particle formation.

While many studies have investigated NPF around the world, only a few have focused on the vertical distribution of these events (Stratmann et al., 2003; Wehner et al., 2010). In view of this, we devised a campaign with the aim to study photochemical episodes, including high $O_3$ levels and NPF in Madrid metropolitan area. In a twin article (Querol et al., 2018) the study of the temporal and spatial variability of $O_3$ is presented. In this work we will focus exclusively on the phenomenology of the NPF events, comparing the aerosol size distribution ~~in~~ at surface level ~~stations in~~at urban, urban background and suburban ~~environments~~stations in Madrid and the outskirts of a residential village 17 km from Madrid~~,~~. We also study the vertical distribution of the events ~~and aloft~~ using airborne instrumentation ~~with surface levels and studying its temporal evolution~~carried by tethered balloons. ~~In a twin article (Querol et al., 2017b) the study of the temporal and spatial variability of $O_3$ is presented.~~

## 2 Methodology

### 2.1 The study area

The Madrid Metropolitan Area (MMA) lies in the center of the Iberian Peninsula at an elevation of 667 m above sea level (a.s.l.). It is surrounded by mountain ranges and river basins that channel the winds in a NE-SW direction. Having an inland Mediterranean climate, winters are cool and summers are hot, and precipitation occurs mainly in autumn and spring. Road traffic and residential heating in winter are the main sources of air pollutants, with small contributions of industrial and aircraft emissions (Salvador et al., 2015).

In summer, the area is characterized by strong convection, which results in PBL heights as high as 3000 m above ground level (a.g.l.), and mesoscale recirculation caused by anabatic and katabatic winds in the surrounding mountain ranges (Plaza et al., 1997, Crespí et al., 1995), which can lead to accumulation of pollutants if the recirculation persists for several days.

Cold and warm advection of air masses associated with the passage of upper level troughs and ridges over the area give rise to a sequence of accumulation and venting periods, respectively. During accumulation periods, pollutants accumulate in the area and concentrations increase for 2-6 days, until a trough aloft brings a cold advection and a venting period starts. For a detailed description of the meteorological context during the campaign see Querol et al. (2018~~7b~~).

A few studies have focused on NPF events in the area. For instance, Gómez Moreno et al. (2011) reported NPF episodes in Madrid to be 'not a frequent phenomenon', since only 63 events per year were detected, 17 % of the total days, occurring mostly in spring and summer. However, Brines et al. (2015) reported both intensive summer and winter NPF episodes at the same station that accounted for 58 % of the time as an annual average, considering the prevalence of nucleation bursts ~~during~~for 2 hours or more. Alonso-Blanco et al. (2017) described the phenomenology of particle shrinking events, i.e. a decline in particle size caused by particle-to-gas conversion, at an urban background station in Madrid (CIEMAT), stating that they occur mainly between May and August in the afternoon, due to either a change in wind direction or the reduction of photochemical processes. Particle shrinkage following their growth is not a common phenomenon but has been observed in a few areas around the world. Yao et al. (2010), Cusack et al. (2013a and 2013b), Young et al. (2013), Skrabalova et al. (2015) and Alonso-Blanco et al. (2017) and references therein, reported shrinkage rates ranging from –1.0 to –11.1 nm $h^{-1}$.

### 2.2 Instrumentation

The data used in this study was collected during a summer campaign in and around Madrid in July 2016. Three air quality supersites were used, ~~two~~ an urban station~~s~~, an urban background station and ~~one~~a suburban station, in addition to a setting in a suburban environment with two tethered balloons that allowed study of the vertical distribution of aerosol and air pollutants. All stations are located within a range of 17 km. A map displaying all locations is shown in Fig. S1.

The CSIC urban station, operative from 9 to 20 July, was located in the Institute of Agricultural Sciences (40°26'25" N, 03°41'17" W, 713 m a.s.l.) in central Madrid. The instrumentation in this station was installed in the sixth floor of the building. $NO_x$ and equivalent black carbon (BC) concentrations were measured with a chemiluminescence based analyzer (Teledyne API, 200EU) and an Aethalometer (AE33, Magee Scientific), respectively. The aerosol number size distribution was measured with a Scanning Mobility Particle Spectrometer (SMPS) (TSI, 3082) equipped with a nano-Differential Mobility Analyzer (DMA), for the size range 8-120 nm, and a Particle Size Magnifier (PSM) (AirModus) in scanning mode for the size range 1.2-~~4~~2.5 nm. PSM data were post-processed using tailored software provided by Airmodus.

The CIEMAT urban background station, operative from 4 to 20 July was located in the outskirts of Madrid, 4 km from the CSIC station (40°27'23" N, 03°43'32" W, 669 m a.s.l.). $NO_x$, $O_3$ and BC concentrations were measured with a

chemiluminescence based analyzer (THERMO 17i), an ultraviolet photometry analyzer (THERMO 49i) and an Aethalometer (AE33), respectively. The aerosol number size distribution was measured with an SMPS (TSI 3080) for the size range 15-660 nm and a 1 nm SMPS (TSI 3938E77) for the size range 1-30 nm. Important discrepancies were observed when merging both SMPS particle size distributions. In order to correct that, we studied the distribution of particles in the coinciding size range (14-31 nm). The daily nanoSMPS size distribution was divided by the daily average of this range. We compared the resulting merged particle size distribution with CPC measurements, to check that there was a good agreement in the total particle concentration. Temperature (4 m a.g.l.), relative humidity (4 m a.g.l.), solar radiation (35 m a.g.l.) and wind speed and wind direction (55 m a.g.l.) were measured at a meteorological tower at the station.

The ISCIII suburban station was located in the Institute of Health Carlos III, in Majadahonda, 15 km from the CSIC station (40°27'27" N, 03°51'54" W, 739 m a.s.l.) and was operative from 4 to 20 July. An SMPS (TSI 3080) measured the aerosol number size distribution in the size range 9-360 nm, and a PSM (AirModus) in scanning mode in the size range 1.2-4.0 nm. PTR-ToF-MS (Ionicon Analytik, PTR-TOF 8000) operating in H3O+ mode was used to measure VOCs. Detailed description of the instrument ~~of the instrument~~ can be found in Graus et al. (2010). Operation procedure of the PTR-ToF-MS is fully described in Querol et al. (2018~~7b~~). Results regarding these measurements are briefly presented in Sect. S1.

TSI instruments at all stations were corrected for diffusion losses and multiple charge losses using the instruments' own software. The measuring conditions were the same at all sites.

Regarding the vertical measurements, two tethered balloons carrying miniaturized instrumentation were based at Majadahonda (MJDH) rugby field (40°28'29.9" N 3°52'54.6" W, 728 m a.s.l.), 17 km from CSIC. 28 flights up to 1200 m a.g.l. were carried out from 11 to 14 July. A miniaturized SMPS (Hy-SMPS) measured the particle size distribution in the range 8-245 nm with a time resolution of 45 s and flow of 0.125 L/min (Lee et al., 2015). However, only particles larger than 10 nm could be detected due to a lower efficiency for finer particles. ~~The instrument was inter-compared with the conventional SMPS (TSI 3080) installed at ISCIII station. The instruments were moderately correlated based on total particle concentration in the size range 9.14-241.44 nm: $N_{MJDH} = 1.3\ N_{ISCIII} - 124.5\ cm^{-3}$; $R^2$=0.47~~ The instrument was intercompared with a TSI-SMPS (Standard DMA with 3776 CPC) for 50-nm monodisperse NaCl particles and polydisperse aerosol (Fig. S2). Particle concentration in the range 3-1000 nm was measured with a miniaturized butanol-based CPC (Hy-CPC). The time resolution was 1 s, and sample flow was 0.125 L/min (Lee et al., 2014). Temperature, relative humidity, pressure, wind speed and wind direction were also measured. The instrumentation was also equipped with a Global Positioning System (GPS). An additional set of the miniaturized instrumentation was placed at surface level for comparison.

### 2.3 Data analysis techniques

Identification of NPF events was made by the method proposed by Dal Maso et al. (2005). After examination of the daily particle size distribution, if the day was classified as an event day we proceeded to calculate growth rates (GR), shrinking rates (SR), condensation and coagulation sinks (CS and CoagS) and formation rates ($J_{Dp}$).

The algorithm proposed by Hussein et al. (2005) was used to fit log-normal modes to the particle size distribution, from which GR were calculated following Eq. (1):

$$GR = \frac{dD_p}{dt}, \quad (1)$$

where $D_p$ are the selected geometric mean diameters corresponding to growing particle modes. Unless stated otherwise, in this work growth rates are calculated for particles growing from 9 to 25 nm. When calculating growth rates with PSM data,

the range was selected accordingly to the measuring range of each instrument (see Sect. 2.2). –SR were calculated analogously when a decrease in the diameter of the fitted modes was observed.

CS, a measure of the removal rate of condensable vapor molecules due to their condensation onto the pre-existing particles (Kulmala et al., 2012), is calculated using Eq. (2):

$$CS = 2\pi D \sum_i \beta_i D_{p,i} N_i \,, \quad (2)$$

where D is the diffusion coefficient of the condensing vapor (here we use $H_2SO_4$), $D_{p,i}$ and $N_i$ are the particle diameter and particle concentration for the size class $i$. $\beta_i$ is the transitional correction factor:

$$\beta_i = \frac{1+K_i}{1+\left(\frac{4}{3\alpha}+0.337\right)K_i+\frac{4}{3\alpha}{K_i}^2}, \quad (3)$$

being K the Knudsen number $K_i = {2\lambda}/{D_{p,i}}$, where λ is the mean free path of the condensing vapor in air.

The formation rates of particles were calculated as a 30 minutes averages, following Eq. (4):

$$J_{Dp} = \frac{dN_{Dp}}{dt} + CoagS_{Dp} \cdot N_{Dp} + \frac{GR}{\Delta D_p} N_{Dp}, \quad (4)$$

where we use 9the PSM measuring range 25 nm for $N_{Dp}$, and CoagS is a quantification of the ability of the preexisting aerosol to scavenge newly formed particles. For its calculation we take the geometric mean diameter of the size ranges 91-25 nm, using a merged PSM and SMPS particle size distribution. CoagS can be calculated using Eq. (5):

$$CoagS_{Dp} = \sum_{D_p'} K\left(D_p, D_p'\right) N_{Dp'} \,, \quad (5)$$

where K is the coagulation coefficient. For a detailed description of the parameters and their derivation, see Kulmala et al. (2012).

A rough estimation of the mixed layer height was determined using Hy-CPC measurements. The top of the mixed layer was considered at an altitude in which particle concentration decreases an order of magnitude quasi-instantaneously and remains constant above. All UFP profiles are included in Querol et al. (2018).

Additionally, bivariate polar plots of concentration have been used to relate wind speed and direction with total particle concentration using PSM data by means of the R package *openair* (Carslaw and Ropkins, 2012).

## 3 Results and discussion

### 3.1 Meteorological context

Figure S3 shows the evolution of temperature, relative humidity, wind speed and wind direction measured at CIEMAT from 5 to 20 July 2016. The evolution of temperatures during this period evidences a succession of accumulation and venting episodes. Rain gauges collected significant precipitation only on 6 July at midnight (not shown).

The balloons field campaign, held from 11 to 14 July, coincided with the start of a venting period, coinciding with the passage of an upper level trough, and the transition to an accumulation period, when the trough has moved to the east of the Iberian Peninsula and a ridge passes over the area of study (see Fig. S4). Maxima and minima temperatures drop, while strong westerly winds predominate until they veer to NE on 12 July 18:00 UTC. High nocturnal wind speed peaks are recorded in this period, often accompanied by a change in wind direction. For detailed information on meteorological parameters during this campaign see Querol et al. (20187b).

### 3.2 Comparison of NPF events at urban and suburban surface stations

In the following discussions, we group CSIC (urban) and CIEMAT (urban background) as urban stations and compare them to ISCIII (suburban). This is because of the availability of data during the period of interest. However, it has to be noted that CSIC is more influenced by traffic than CIEMAT, therefore it is more representative of urban environments, and for this reason CSIC data is chosen when possible. 18 NPF episodes have been identified on a total of ~~12~~ 7 days throughout the campaign. In Table 1 a summary of these events is presented. Out of these, a total of 14 events on 6 days had simultaneous data available for at least one of the urban stations (CSIC, CIEMAT) and the suburban station (ISCIII). These episodes, marked with a star in Table 1, are selected for further analysis in this section. Figure 1 represents the aerosol particle size distribution of the selected episodes (12-18 July 2016).

#### 3.2.1 Episode characteristics

In the selected episodes, intensive daytime nucleation and subsequent condensational growth processes took place simultaneously at urban and suburban stations, located 17 km apart, and accordingly we classify these as regional NPF episodes. Being all stations differently influenced by traffic (influenced, slightly and not influenced by traffic), we can affirm that these episodes are regional events and not representative of primary emissions. Otherwise, we would observe significant differences at our stations. Additional arguments are the fact that number concentrations of sub-25 nm particles peak at noon, when BC levels are at their minimum, as well as concentration of particles measured by PSM being higher at the suburban station, compared to the urban station, implying that the particles are not originated from traffic sources.

~~Nonetheless, some differences exist between urban and suburban events.~~

At urban stations particles of the order of 10 nm are detected throughout the day, even at night time. Conversely, at the suburban station such small particles are only detected during daytime. Additionally, during some days a very intense short nucleation burst is registered around midnight local time at urban stations that are not detected at the suburban station. This phenomenon ~~will be~~ is analyzed ~~later~~ in ~~this~~ section 3.4.2.

Despite the detection of sub-10 nm particles as early as 04:00 UTC (06:00 local time) at the urban stations, only after around 09:00 UTC the growth of the particles is observed, occurring roughly at the same time in both urban and suburban stations. Newly formed particles grow until they have reached sizes of up to 50 nm, usually around 13:00 UTC (15:00 local time). After this, shrinkage is observed on 10 days, corresponding to 71 % of the days with available data. Consequently, the evolution of the particle size distribution is arc-shaped in these cases.

~~A further interesting feature is the presence of an additional Aitken mode on most days. Usually in the size range 50–100 nm, reaching 110 nm in some cases, this mode doesn't correspond to newly formed particles, but it follows a parallel evolution (condensational growth and potential shrinkage). When looking at the evolution of aerosol size distributions on consecutive days, it is possible to see a connection between this 50–100 nm mode and the distribution of the previous days. The nucleated and grown mode of one day is still present the following day and it continues to grow until it eventually fades away. In some occasions the Aitken mode can be tracked for two or more consecutive days, alternating stages of growth and shrinkage.~~

~~The start of the shrinking phase coincides with a marked increase in wind speed, therefore it is associated with dilution and possibly with a change in air masses. Figure 2 shows the shrinkage rates according to the starting diameter of the shrinking particles and the stations. Data used for this figure including start and end times and diameters is included in Table S1. The calculated shrinkage rates for particles with a starting diameter below 40 nm range from –1.1 to –8.0 nm $h^{-1}$. For particles in~~

~~the Aitken mode above 40 nm the values fall between -4.9 and -20.5 nm $h^{-1}$. Finally, particles that have reached the accumulation mode (i.e., particles greater than 100 nm) after their growth can shrink much faster, with values reaching -48.7 nm $h^{-1}$, the median being -12.7 nm $h^{-1}$. The results confirm that shrinkage is a regional phenomenon in the Madrid area, as already suggested by Alonso-Blanco et al. (2017), the processes being faster in the suburban station compared to the urban station. It is also observed that particles shrink faster the larger the starting diameter is.~~

It should be noted that nucleation episodes coincide in time with the early increases in $O_3$ concentrations in the morning, whereas the occurrence of maximum $O_3$ concentration (120 to 150 µg $m^{-3}$ hourly daily maxima between 14:00 and 16:00 UTC; see Fig. S5) takes place during the UFP growth stage, since oxidation of VOCs and inorganic gases is also accelerated with photochemistry and the presence of $O_3$ and OH radicals, among others (Coleman et al., 2008; Wang et al., 2017; Saiz-Lopez et al., 2017). ~~NPF leads to maximal UFP concentrations around midday in all stations, which are recorded in coincidence with very low BC levels.~~

### 3.2.2 Comparison of GR, $J_{19}$, CS and $CoagS_9$

For the observed daily regional NPF events, GR for the nucleation mode, $J_{19}$, CS and $CoagS_9$ have been determined using PSM and SMPS aerosol size distribution measurements. Here, the growth rate is calculated from the time of detection of the smallest mode until either the particle reaches 25 nm or it stops growing before reaching that size. We considered only the events that are observed simultaneously at the suburban station and at least at one urban station (highlighted in Table 1). Figure 2~~4~~ shows the growth rates presented in Table 1 according to urban and suburban surface stations. GR regarding the vertical measurements are discussed in the following section due to differing sampling periods. Growth rates were significantly higher at the suburban station, ranging 2.9-10.0 nm $h^{-1}$ with a median value of 5.8 nm $h^{-1}$, compared to values ranging 2.0-3.9 nm $h^{-1}$ with a median value of 2.7 nm $h^{-1}$ at the urban stations. This is consistent with the observed GR by Alonso-Blanco et al. (2017), ranging 1.4-10.6 nm $h^{-1}$ at CIEMAT.

The GR calculated in this study are also consistent with those observed in other urban and suburban areas. Kulmala et al. (2004) concluded that typical growth rates are 1-20 nm $h^{-1}$ in mid-latitudes. In particular, Stolzenburg et al. (2005) observed GR ranging 2.4-8.5 nm $h^{-1}$ in regional events in an urban environment in Atlanta, US. Qian et al. (2007) reported regional events with median GR of 5.1 nm $h^{-1}$ in an urban environment in St. Louis, US. Ahlm et al. (2012) reported average GR of 7.3 nm $h^{-1}$ at Bakersfield, US. Manninen et al. (2010) characterized NPF events in 12 European sites. Cabauw (The Netherlands) and San Pietro Capiofume (Italy), are stations located in environments comparable to that in our suburban station, ISCIII. For these stations the observed median growth rates were 7-8 nm $h^{-1}$, corresponding well with our calculated GR in the suburban station.

Figure 3~~5~~ shows the average daily cycles of ~~total~~ particle concentration in the size range 9-25 nm ($N_{9-25}$), total particle concentration measured by the PSM ($N_{>2.5}$), CS and $CoagS_9$ during the regional NPF events at urban and suburban stations. ~~$N_{9-25}$, a~~Average $N_{9-25}$ daily mean values are 3.7 x $10^3$ $cm^{-3}$ and 2.2 x $10^3$ $cm^{-3}$ at urban and suburban stations, respectively. The difference in number concentration in urban and suburban stations could explain the difference in GR: if we consider that the vapor source is the same at all locations, it would be divided in bigger number of particles at the urban stations, thus giving slower GR. $N_{>2.5}$ have average daily mean values of 1.6 x $10^4$ $cm^{-3}$ and 2.1 x $10^4$ $cm^{-3}$ at urban and suburban stations, respectively. CS and $CoagS_9$ have average daily mean values of 3.4 x $10^{-3}$ $s^{-1}$ (2.5 x $10^{-3}$ $s^{-1}$ at the suburban station) and 2.4 x $10^{-5}$ $s^{-1}$, respectively. After dawn, anthropogenic activities start, and $N_{9-25}$, $N_{>2.5}$, CS and $CoagS_9$ start to increase at the same time, both in urban and suburban environments. Around 07:00 UTC, once the morning traffic rush diminishes, $N_{9-25}$~~-~~, $N_{>2.5}$ and the sinks increase more slowly; moreover, ~~$N_{9-25}$~~total particle concentration decreases in the suburban station, indicating that in this environment the impact of the traffic emissions in total particle concentration is smaller than near the city center,

as expected. Shortly after, at 09:00 UTC the photochemical processes are strong enough to start NPF, as suggested by the increase in ~~$N_{9-25}$~~particle concentrations, while the sinks get to a relative minimum. $N_{9-25}$ reaches its maximum at midday (9 x $10^3$ $cm^{-3}$ and 5 x $10^3$ $cm^{-3}$ at the urban and suburban stations, respectively), and then decrease because the particles start growing to diameters greater than 25 nm, adding to the sinks, which increase gradually until the evening. NPF leads to maximal UFP concentrations around midday in all stations, as suggested by the peak in $N_{>2.5}$, which is recorded in coincidence with very low BC levels (see Figs. S5 and S6). Around 19:00 UTC the effect of the afternoon traffic rush is evident, the variables evolving equivalently to that in the morning. Finally, at 23:00 UTC a sharp and short increase in $N_{9-25}$ is observed, associated with the aircraft emissions discussed ~~above~~in Sect. 3.4.2.

~~Total formation rates of 9-25 nm particles ($J_9$) were calculated from SMPS data of urban and suburban stations. Figure 6 summarizes the daily evolution of $J_9$ for the days in which an event is detected at both urban and suburban stations. Median hourly maximum values are registered at 10:00-12:00 UTC (2.0 $cm^{-3}$ $s^{-1}$) at the urban stations, and at 13:00-14:00 UTC (1.1 $cm^{-3}$ $s^{-1}$) at the suburban station. Median values are generally higher at the urban stations, especially during the central hours of the day. The ranges are also broader at the urban stations, with ranges of up to 4 $cm^{-3}$ $s^{-1}$ at midday and outliers reaching 5 $cm^{-3}$ $s^{-1}$ at night, which agree with the observed nocturnal peaks at CSIC. The fact that $J_9$ is higher at the urban stations is probably linked to higher traffic emissions (20-30 nm, Brines et al., 2015) in the city, and not related with higher nucleation rates, since PSM measurements indicate lower concentrations of 1.2-4 nm particles compared to the suburban measurements (Figure S4). The calculated formation rates agree with those reported in other studies (see Kulmala et al. 2004 and references therein), ranging 0.01-10 $cm^{-3}$ $s^{-1}$ during regional events around the world.~~

Growth rates ($GR_{PSM}$) and total formation rates of 1.2-4.0 nm particles ($J_1$) were calculated from PSM data at CSIC and ISCIII stations. $GR_{PSM}$ were calculated from 11 to 18 July 2016, averaging 4.3 nm $h^{-1}$ at the urban station and 3.7 nm $h^{-1}$ at the suburban station. $J_1$ were calculated only for the days in which NPF is identified. The results for these days are included in Table 1. Average $J_1$ values are higher at the urban station (8.9 $cm^{-3}$ $s^{-1}$) compared to the suburban station (5.3 $cm^{-3}$ $s^{-1}$). Concentrations of 1.2-4.0 nm particles are lower at the urban station (Figure S6), which could lead to lower formation rates. However, the coagulation sink is greater at the urban station, as discussed before, which contributes to the second factor in Eq. (4). It has to be noted that only 3 days of PSM data were available for NPF events at the urban station. A longer dataset could lead to different results.

The average values of the formation rates agree with those reported at similar stations around the world. For instance, Woo et al. (2001) reported $J_3$ ranging 10-15 $cm^{-3}$ $s^{-1}$ in Atlanta, US. Wehner and Wiedensohler (2003) reported average $J_3$ of 13 $cm^{-3}$ $s^{-1}$ in Leipzig, Germany. Hussein et al. (2008) reported nucleation rates ($D_p$<25 nm) ranging 2.1-3.0 $cm^{-3}$ $s^{-1}$ in summer in Helsinki.

### ~~3.2.3 PTR-ToF-MS measurements~~

~~Among the 152 ions identified with the PTR-ToF-MS, only 3 exhibit temporal trends that might be relevant in the growth processes of NPF (Fig. S6). Two highly oxygenated ions, $C_4H_4O_3H^+$ (m/z 101.023) and $C_2H_4O_3H^+$ (m/z 77.023), and $NO_2^+$ (m/z 45.9924) presented evolutions parallel to those of the particle diameter, i.e. the concentration of these ions increased simultaneously with the increase of particle diameter, and growth stopped when the concentration of the ions decreased (Fig. S6). This is observed also on days in which there is no particle formation but there is particle growth. Thus, the parent molecules of these ions are not linked to particle formation, but they would most probably contribute to particle growth. The fragment $C_4H_4O_3H^+$ has, to the best of our knowledge, only been reported once over an orange grove in California (Park et al., 2013) and is most probably from secondary origin considering both its diurnal variation and oxidation state. It contains sufficient carbon atoms~~

and oxygen functional groups to likely partition into the condensed phase. $NO_2^+$ and $C_2H_4O_3^+$ are known fragments of peroxyacetyl nitrate (PAN) (de Gouw et al., 2003), but $NO_2^+$ can also arise from the fragmentation of a wide range of peroxynitrates ($ROONO_2$) or alkyl and multifunctional nitrates ($RONO_2$) (Aoki et al., 2017; Duncianu et al., 2017). While the uptake of PAN on particles can be considered as negligible (Roberts, 2005), higher molecular weight organonitrates are more likely to partition onto the particle phase. Thus, the particles growth appears to be driven by the uptake of secondary organic compounds. More precisely, in an urban atmosphere such as Madrid characterized by high $NO_2$ concentrations, the formation of organonitrates and/or peroxynitrates could play an important role in the particle growth processes.

### 3.2.4 Nocturnal UFP peaks

There are other interesting events taking place during night time. From 6 to 11 July and 17 to 19 July, high concentrations of 1.2 4 nm particles are registered shortly after sunset for several hours, simultaneously at urban and suburban stations (Fig. S7). BC, NO and $NO_2$ concentrations also increase during that time (see Fig. S5). Therefore, these processes are probably related to local traffic emissions and the decrease of the mixing layer after sunset. On the other hand, from 12 to 14 July high concentrations of sub 25 nm particles are also detected, but only registered at the urban stations around 23:00 UTC. These are sudden, shorter and more intense, with concentrations greater than $10^5$ $cm^{-3}$. They appear as intense bursts that last one hour or less, with no subsequent growth. Unlike the regional events, these are not accompanied by simultaneous high BC or NO concentrations, thus they are not linked to traffic emissions, although $NO_2$ levels are significant. Furthermore, these episodes occur outside local traffic rush hours, and are registered together with strong NE winds, which suggest that they might be transported and not formed locally.

In order to determine the origin of these sub 25 nm particles, bivariate polar plots of concentration have been used to relate wind speed and direction measured at CIEMAT with total particle concentration of 1 4 nm particles, BC, $NO_2$ and NO measured at CSIC, separately analyzing daylight and night time periods (Fig. 3). These plots must be carefully interpreted, since the color scale only represents the average value for a given wind speed and direction. The results are consistent with what we previously stated: the highest nocturnal 1 4 nm particle concentrations are linked with strong winds from NE direction. Air masses transported from this direction have the lowest BC levels, and moderate $NO_2$ concentrations. NO concentrations are insignificant at nighttime considering any direction, probably because of titration due to the high concentrations of $O_3$ observed during daytime. The airport Adolfo Suárez Madrid Barajas is located NE of the city, 12 km from of the urban stations (see Fig. S1). With more than 34000 operations in July 2016 (AENA, 2016), it is the sixth busiest airport in Europe. Other studies have linked aircraft emissions with nucleation bursts without growth (Cheung et al., 2011, Masiol et al., 2017), having the particle size distribution of the aircraft emissions in their area of study a characteristic mode peak at around 15 nm (Mazaheri et al., 2009). Considering that the airport of Madrid is relatively busy also at nighttime, and in regard of our results, we assume that the observed local nocturnal nucleation mode events are associated with transported aircraft emissions. Since the airport is located almost 30 km to the E of ISCIII, the emissions would be significantly diluted by the time they arrive at that station, in comparison with the considered urban stations.

### 3.3 Vertical distribution of NPF events

#### ~~3.2.5~~3.3.1 UFP concentrations

Querol et al. (2018~~7b~~) studied the vertical profiles of UFP and O3 concentrations measured during the campaign using the balloon soundings at Majadahonda. UFP concentrations are homogeneous throughout the mixing layer and present a sharp decrease at the top. As the day progresses, the convection is more effective and high UFP levels reach higher altitudes, as the mixing layer heightens~~. This suggests that UFP fluxes are bottom up~~. Moreover, the concentrations tend to increase until midday. Afterwards, they remain constant or slightly decrease, always showing homogeneous levels from surface levels to the top of the PBL. Concentrations of UFP markedly increased from 11 to 14 July, both at surface and at upper levels. This is consistent with the observed decrease of the convective activity in that period, evidenced by a decrease in temperatures, but also with an increase in the formation rates, calculated in this study. Therefore, the increase in particle concentration is probably the result of both a decline in PBL height and more intense nucleation episodes.

#### ~~3.2.6~~3.3.2 Particle size distribution and NPF episodes

The NPF events described in Sect. 3.2 that took place between 12 and 14 July were not only detected at surface level but also in upper layers with the balloons soundings in Majadahonda. However, the measurements were not continuous, since the balloons could not be operated safely if the wind speed was above 8 m $s^{-1}$ at any vertical level.

Figure ~~4~~7 shows the fitted modes to the particle size distribution measured in the soundings on 12 July. The fact that sub-40 nm particles are not detected at the higher levels of the first flights suggests that convection is not very effective yet, and the sounding goes through different atmospheric layers, most likely the mixed layer and the residual layer. In the residual layer Aitken-mode particles formed on previous days prevail (Stull, 1988). The interphase between the mixed layer and the residual layer, i.e. the mixed layer height, has been derived using the UFP vertical profiles (see Querol et al., 2018). ~~would be around 1300 m at 7:00 UTC, 1500 m at 9:00 UTC and higher than 1800 m from 10:00 UTC.~~ From 10:00 UTC onwards, once the convection has fully developed, the mixed layer covers all the sounding and we see a homogeneous distribution at all levels, which is also comparable to those recorded with the instrumentation measuring at the surface. This agrees with the fact that UFP are homogeneously distributed in the mixed layer and are detected at higher altitudes as the mixed layer rises ~~fluxes are bottom up, as we stated in Sect. 3.3.1~~.

In the early morning the size distribution is dominated by a 60 nm mode at all altitudes, which grows to 100 nm at 11:00 UTC. Even though it is detected at all levels, the mode slightly decreases its size when the sounding ascends above the mixed layer limit, more clearly visible on the second flight, around 9:00 UTC. This result suggests that there are less vapors in the residual layer, which inhibits particle growth, whereas the mixed layer is more polluted, thus the particles can grow faster. The growth rates calculated for this mode were 1.8 nm $h^{-1}$ in the residual layer, and 7.3 nm $h^{-1}$ in the mixed layer. The concentration and size of the Aitken mode decrease after midday, which might be related to ~~a change of air masses~~an increase of wind speed that entailed dilution and evaporation, leading to shrinking of the particles. Because of the increase in wind speed the balloons could not be safely operated, and no additional flights were made on that day.

Moreover, during the morning we observed particles growing inside the mixing layer from 10 nm at 7:00 UTC, to 30 nm at midday~~, with a growth rate of 3.5 nm $h^{-1}$~~. This mode is observed simultaneously at ISCIII and therefore we consider it for calculation. The growth rate obtained is 3.5 nm $h^{-1}$. The fact that the growth rate is the same throughout the mixing layer even though we expect VOCs to be higher near the surface upholds the assumption that the convection is very efficient, and the entire layer is well-mixed. After 13:00 UTC, because of the ~~change in air masses~~increase in wind speed particles start to

shrink. While concentrations were not as high as other episodes, the evolution is remarkably similar to the NPF event measured at the same time at ISCIII, which had a growth rate of 3.0 nm $h^{-1}$.

The size distribution and the corresponding fitted modes for the soundings made on 13 July are presented in Fig. ~~8~~5. Although the balloons could not fly until 10:30 UTC for safety reasons, ~~3~~at least 2 modes are detected from early morning at the sounding location. ~~The accumulation mode grows from 156 nm at 07:00 UTC to 200 nm at 10:00 UTC, with a growth rate of 13.3 nm $h^{-1}$. After that time the particles have grown beyond the detection limit. This mode is also detected at ISCIII, growing 13.7 nm $h^{-1}$, following a similar evolution, but not at CSIC since this size range is beyond the detection limit of the SMPS.~~ A~~nother~~ mode starting roughly at 40 nm at ~~09~~07:00 UTC grows to 100 nm at 15:00 UTC. With a growth rate of 8.5 nm $h^{-1}$, this mode was detected at all altitudes once the soundings started, indicating that the convection was already effective by 10:30 UTC and all the measured altitudes were completely mixed, leading to a homogeneous particle distribution throughout the soundings. This mode is the prolongation of the Aitken mode detected the day before, which shrank from midday until the following morning. It is also detected at ISCIII and CSIC, with growth rates of 7.5 nm $h^{-1}$ and 6.9 nm $h^{-1}$. A nucleation mode grows from the detection limit of the instrument, around 10 nm at 08:30 UTC to 40 nm at 15:00 UTC. Comparing with other stations, we considered this mode only after 9:00 UTC, and calculated the growth rates from that time. We consider this a regional NPF event, since the start of the particle growth is registered simultaneously at all the stations. The growth rates at the sounding location, ISCIII and CSIC are 5.3 nm $h^{-1}$, 4.6 nm $h^{-1}$ and 2.0 nm $h^{-1}$, respectively.

Finally, Fig. ~~6~~9 shows the particle size distribution and fitted modes for the soundings made on 14 July. Correspondingly, in Fig. 7~~10~~ the vertical distribution of particles for some of the soundings is presented. The earliest soundings revealed the existence of a residual layer aloft. In order to verify this result two constant altitude flights were made during the morning. The extension of the wire was not modified during these flights. However, changing wind conditions varied slightly the altitude of the instruments. The altitude was chosen so that the instruments remained initially outside the mixing layer, i.e. inside the residual layer. As the insolation increased, so did the altitude of the mixing layer, until it reached the altitude at which the balloons were positioned. As the mixing layer reached the balloons, total particle concentration sharply increased from $4x10^3$ to $2x10^4$ $cm^{-3}$, demonstrating that newly-formed particles ~~flow upwards and~~ remain inside the mixing layer.

According to the abrupt decline in particle concentration, the boundary between the mixing and residual layers was located at 1000 m at 09:00 UTC, 1200 m at 10:00 UTC, 1350 m at 11:00 UTC and beyond 1800 m after 12:00 UTC. This can be taken as an indicator of the effectiveness of convection, meaning that after 12:00 UTC all the measured particle population was well mixed throughout the sounding range. Inside the residual layer particles had a slower growth rate (0.5 nm $h^{-1}$ compared to 8.45 nm $h^{-1}$ for the 40 nm mode – note that due to the use of a log-scale this might be unnoticeable visually), and no particles smaller than 20 nm were observed.

~~The Aitken mode particles observed on the previous days prevailed and had grown to 170 nm at 08:00 UTC, reaching the detection limit (240 nm) by 10:00 UTC. Furthermore, n~~Nucleation mode particles were detected exclusively inside the mixing layer from 08:00 UTC to 12:00 UTC, whereas growth was only observed from 09:00 to 11:00 and from 12:00 onwards. The time spacing between both growing periods coincides with a marked decrease in wind speed. During the first period growth rates at the sounding station, ISCIII and CSIC were 6.2, 5.4 and 1.4 nm $h^{-1}$, respectively. However, during the second stage particles grew faster at the urban station (8.6 nm $h^{-1}$) than at the sounding location (4.5 nm $h^{-1}$). As the latter is a suburban environment, this contrasts with the results obtained in Sect. 3.2.2. This fact could be explained by the veer of NE winds to weaker southerly winds in Madrid, which is not observed in Majadahonda.

Overall, the soundings revealed that there is simultaneous growth and shrinking of ~~3 different modes:~~ nucleation and~~,~~ Aitken ~~and accumulation~~ modes, and that ~~all~~ both of them grow and shrink at ~~very~~ different rates. This was also observed in the surface measurements when comparing urban and suburban stations (see Sect. 3.~~2~~2.~~2~~2). ~~This observation demonstrates that~~

~~there are plenty of semivolatile vapors that condense onto and evaporate from the accumulation mode in this environment. Furthermore, the fact that the Aitken and nucleation modes have slower growth, implies that there is either less vapors that condense on the accumulation mode (they would need to be less volatile), or the smaller particles cannot uptake as much of the vapors as the larger, due to particle phase chemistry (Apsokardu and Johnston, 2017). This phenomenon has been rarely reported in ambient air.~~

## 3.4 Other observations

### 3.4.1 Prevalence of particles and shrinkage

A further interesting feature is the presence of the Aitken mode on most days. Usually in the size range 50-100 nm, reaching 110 nm in some cases, this mode doesn't correspond to newly formed particles, but it follows a parallel evolution (condensational growth and potential shrinkage). When looking at the evolution of aerosol size distributions on consecutive days, it is possible to see a connection between this 50-100 nm mode and the distribution of the previous days. The nucleated and grown mode of one day is still present the following day and it continues to grow until it eventually fades away or grows beyond the detection limits of the instruments. In some occasions the Aitken mode can be tracked for two or more consecutive days, alternating stages of growth and shrinkage.

The start of the shrinking phase coincides with a marked increase in wind speed (Fig. S7), therefore it is associated with dilution, which favors the evaporation of semi-volatile vapors, resulting in a decline in particle diameter and concentrations, as observed in most cases. Figure 8 shows the shrinkage rates according to the starting diameter of the shrinking particles and the stations. Data used for this figure including start and end times and diameters is included in Table S1. The calculated shrinkage rates for particles with a starting diameter below 40 nm range from -1.1 to -8.0 nm $h^{-1}$. For particles in the Aitken mode above 40 nm the values fall between -4.9 and -20.5 nm $h^{-1}$. The results confirm that shrinkage is a regional phenomenon in the Madrid area, as already suggested by Alonso-Blanco et al. (2017), the processes being faster in the suburban station compared to the urban station. It is also observed that particles shrink faster the larger the starting diameter is.

### 3.4.2 Nocturnal UFP peaks

There are other interesting events taking place during night time. From 6 to 11 July and 17 to 19 July, high concentrations of 1.2-4 nm particles are registered shortly after sunset for several hours, simultaneously at urban and suburban stations (see Fig. 1). BC, NO and $NO_2$ concentrations also increase during that time (see Fig. S5). Therefore, these processes are probably related to local traffic emissions and the decrease of the mixing layer after sunset. On the other hand, from 12 to 14 July high concentrations of sub-25 nm particles are also detected, but only registered at the urban stations around 23:00 UTC. These are sudden, shorter and more intense, with concentrations greater than $10^5$ $cm^{-3}$. They appear as intense bursts that last one hour or less, with no subsequent growth. These are not accompanied by simultaneous high BC or NO concentrations, thus they are not linked to traffic emissions, although $NO_2$ levels are significant. Furthermore, these episodes occur outside local traffic rush hours, and are registered together with strong NE winds, which suggest that they might be transported from a stationary source and not formed locally. To better support this hypothesis, Fig. S8 shows PSM data together with wind direction and wind speed, showing that the episodes coincide with strong NE winds, and that there are not episodes with low UFP concentrations with the same wind conditions.

In order to determine the origin of these sub-25 nm particles, bivariate polar plots of concentration have been used to relate wind speed and direction measured at CIEMAT with total particle concentration of 1.2-2.5 nm particles, BC, $NO_2$ and NO measured at CSIC, separately analyzing daylight and night time periods (Fig. 9). These plots must be carefully interpreted, since the color scale only represents the average value for a given wind speed and direction. The results are consistent with what we previously stated: the highest nocturnal 1.2-2.5 nm particle concentrations are linked with strong winds from NE direction. Air masses transported from this direction have the lowest BC levels, and moderate $NO_2$ concentrations. NO concentrations are insignificant at nighttime considering any direction, probably because of titration due to the high concentrations of $O_3$ observed during daytime. The airport Adolfo Suárez Madrid-Barajas is located NE of the city, 12 km from of the urban stations (see Fig. S1). With more than 34000 operations in July 2016 (AENA, 2016), it is the sixth busiest airport in Europe. Other studies have linked aircraft emissions with nucleation bursts without growth (Cheung et al., 2011, Masiol et al., 2017). Considering that the airport of Madrid is relatively busy also at nighttime, and in regard of our results, we assume that the observed local nocturnal nucleation mode events are associated with transported aircraft emissions. Since the airport is located almost 30 km to the E of ISCIII, the emissions would be significantly diluted by the time they arrive at that station, in comparison with the considered urban stations.

## 4 Conclusions

We investigated the phenomenology of regional and secondary New Particle Formation (NPF) episodes in central Spain. To this end we set up 3 supersites (an urban, an urban background and a suburban) 17 km away in and around Madrid. We were able to characterize 6 NPF events, and in all cases the evolution of the particle size distribution (PSD) was very similar at all stations: around sunrise nucleation mode particles appear and start growing and in the afternoon a decline in particle sizes, i.e. shrinkage, is observed. The regional origin of the NPF is supported by the simultaneous variation in PSD in the nucleation mode and particle number concentrations, growth and shrinkage rates. Furthermore, temporal evolutions of condensation and coagulation sinks (CS and CoagS) were similar at all stations, having minimum values shortly before sunrise and increasing after dawn towards the maximum value after midday in the early afternoon. In spite of the 17 km scale simultaneous processes affecting particle number concentrations, the following relevant differences between urban and suburban stations were observed: i) the urban stations presented larger formation rates and smaller growth rates as compared to the suburban stations; ii) in general, the sinks were higher at the urban stations.

Regarding the vertical soundings of the NPF events, we observed that in the early morning the vertical distribution of newly formed particles is differentiated in two layers. The lower layer (mixed layer, ML) in which convection is effective, is well-mixed and has a homogeneous PSD. This ML heightens throughout the day, as insolation is more pronounced, extending beyond the sounding limits around midday. NPF occurs throughout this ML, and growth rates and concentrations are homogeneous. The upper layer is a stable residual one (RL) in which particles formed or transported the previous days prevail. In the RL growth is inhibited or even completely restrained, compared with the same particles in the ML. Overall, the soundings demonstrate that particles are formed inside the ML, but they can prevail and be displaced and stored at upper levels and continue to evolve on following days.

In this campaign we could not measure in the earliest stages of NPF due to safety requirements of the balloon flights early in the morning. We think it is important for future work to carry out soundings during the nucleation phase of the episodes. However, miniaturized instruments able to measure smaller particles would be needed, which are not available at the present time. This would allow us to determine whether secondary NPF takes place throughout the ML or occurs at the surface and is transported upwards by convection afterwards. If the former were true, then locations with high ML could produce more

secondary particles than we have considered, and they could affect a larger population, or influence climate to a greater extent.

Additionally, a few nocturnal bursts of nucleation mode particles were observed in the urban stations, which could preliminarily be related with aircraft emissions transported from the airport of Madrid.

We cannot determine whether the NPF episodes were triggered by the pollution generated in the city that extended to the region, or the events are caused by a broader phenomenon. In either way, it can be concluded that in summer the particle number concentrations are dominated by NPF in a wide area. The impact of traffic emissions on concentrations of UFP is much smaller than those of NPF, even near the city center where the pollution load is at the highest. This result is in line with other studies performed in cities from high insolation regions (e.g. Kulmala et al., 2016). Given the extent of the episodes, the health effects of NPF can affect a vast number of people, considering that the Madrid metropolitan area with more than 6 million inhabitants is the most populated area in Spain, and one of the most populated in Europe (UN, 2008). For this reason, we believe that the study of health effects related to newly-formed particle inhalation is crucial.

~~A total of 6 intensive regional NPF episodes were detected simultaneously at urban and suburban stations located within a 17 km radius in Madrid. The evolution of the size distribution was very similar at all stations: around sunrise nucleation mode particles appear and start growing and in the afternoon a decline in particle sizes, i.e. shrinkage, is observed. The shrinkage can be related to a change in air masses as suggested by the meteorological data. On most days one or more distinct modes were detected – in the Aitken or accumulation ranges – which can be tracked to previous and subsequent days. This implies that particles formed and grown one day can prevail for two or more days in the region if the meteorological conditions are favorable. Some relevant differences between urban and suburban stations were observed. The urban stations presented larger formation rates and smaller growth rates as compared to the suburban stations. Additionally, a few nocturnal bursts of nucleation mode particles were observed in the urban stations, which could be related with aircraft emissions transported from the airport of Madrid. CS and CoagS evolutions were similar at all stations, having minimum values shortly before sunrise and increasing after dawn towards the maximum value after midday in the early afternoon. In general, the sinks were higher at the urban stations. Formation rates were also larger in the urban stations, which might be related to traffic emissions that were considered in the size range used for the calculations.~~

~~We cannot determine whether the NPF episodes were triggered by the pollution generated in the city that extended to the region, or the events are caused by a broader phenomenon. In either way, it can be concluded that in summer the particle number concentrations are dominated by NPF in the area of study. The impact of traffic emissions on concentrations of UFP is much smaller than those of NPF, even near the city center where the pollution load is higher. This result is in line with other studies (e.g. Kulmala et al., 2016). Given the extent of the episodes, the health effects of NPF can affect a vast number of people, considering that the Madrid metropolitan area with more than 6 million inhabitants is the most populated area in Spain, and one of the most populated in Europe (UN, 2008). For this reason, we believe that the study of health effects related to newly-formed particle inhalation is crucial.~~

~~Regarding the vertical soundings of the NPF events, we observed that in the early morning the vertical distribution of newly formed particles is differentiated in two layers. The lower layer, in which convection is effective, is well-mixed and has a homogeneous particle size distribution. This layer heightens throughout the day, as insolation is more pronounced, extending beyond the sounding limits around midday. NPF occurs throughout this layer, and growth rates and concentrations are homogeneous. The upper layer is a stable residual one in which particles formed or transported the previous days prevail. In the residual layer growth is inhibited or even completely restrained, compared with the same particles in the mixed layer.~~

~~Overall, the soundings demonstrate that the flux of ultrafine particles has an upward direction and that particles are formed at surface levels, but they can prevail and be displaced and stored at upper levels and continue to evolve on following days.~~

~~Both at surface and aloft we detected growth and shrinkage of the nucleation, Aitken and accumulation modes, which had very different growth and shrinking rates. This suggests that there are vapors that can condense onto and evaporate from the accumulation mode, which has been rarely documented to this day.~~

~~In this campaign we could not measure in the earliest stages of NPF due to safety requirements of the balloon flights early in the morning. We think it is important for future work to carry out soundings during the nucleation phase of the episodes. However, miniaturized instruments with greater resolution would be needed, which are not available at the present time. This would allow us to determine whether particle formation takes place throughout the mixing layer or occurs at the surface and is transported upwards by convection afterwards. If the former were true, then locations with high PBL could produce more particles than we have considered, and they could affect larger populations if they were transported to surface levels, or affect the climate to a greater extent, since newly formed particles can be activated as cloud condensation nuclei once they grow beyond 50 nm, thus affecting the radiative balance of the Earth.~~

## Acknowledgments

This work was supported by the Spanish Ministry of Agriculture, Fishing, Food and Environment, the Ministry of Economy, Industry and Competitiveness, the Madrid City Council and Regional Government, FEDER funds under the project HOUSE (CGL2016-78594-R), the CUD of Zaragoza (project CUD 2016-05), the Generalitat de Catalunya (AGAUR 2017 SGR44) and the Korean Ministry of Environment through "The Eco-Innovation project". The funding received by ERA-PLANET (www.era-planet.eu), trans-national project SMURBS (www.smurbs.eu) (Grant agreement No. 689443), and support of Academy of Finland via center of excellence in Atmospheric sciences are acknowledged. These results are part of a project (ATM-GTP/ERC) that has received funding from the European Research Council (ERC) under the European Union's Horizon 2020 research and innovation program (Grant agreement No. 742206). Authors also acknowledge the Doctoral program of Atmospheric Sciences at the University of Helsinki (ATM-DP). M.K. acknowledges the support by the Academy of Finland via his Academy Professorship (no. 302958). We also thank the City Council of Majadahonda for logistic assistance, and Instituto de Ciencias Agrarias, Instituto de Salud Carlos III, Alava Ingenieros, TSI, Solma Environmental Solutions, and Airmodus for their support.

## References

AENA, 2016. Statistical report on passenger, aircraft movement and cargo traffic, July 2016. http://www.aena.es/csee/ccurl/586/802/07.Estadisticas_Julio_2016.pdf.

Ahlm, L., Liu, S., Day, D.A., Russell, L.M., Weber, R., Gentner, D.R., Goldstein, A.H., Digangi, J.P., Henry, S.B., Keutsch, F.N., Vandenboer, T.C., Markovic, M.Z., Murphy, J.G., Ren, X., Scheller, S.: Formation and growth of ultrafine particles from secondary sources in Bakersfield, California. Journal of Geophysical Research Atmospheres 117. doi:10.1029/2011JD017144, 2012.

~~Alam, A., Shi, J.P., Harrison, R.M.: Observations of new particle formation in urban air. J. Geophys. Res. 108, 4093, doi:10.1029/2001JD001417, 2003.~~

Alonso-Blanco, E., Gómez-Moreno, F. J., Núñez, L., Pujadas, M., Cusack, M., Artíñano, B.: Aerosol particle shrinkage event phenomenology in a South European suburban area during 2009–2015, Atmos. Environ. 160, 154-164, 2017.

Apsokardu, M. J., and Johnston, M. V.: Nanoparticle Growth by Particle Phase Chemistry. Atmos. Chem. Phys. Discuss. doi:10.5194/acp-2017-529, 2017.

Beddows, D.C.S., Harrison, R.M., Green, D.C., Fuller, G.W.: Receptor modelling of both particle composition and size distribution from a background site in London, UK. Atmos. Chem. Phys. Discuss. 15, 10123-10162, 2015.

Betha, R., Spracklen, D.V., Balasubramanian, R.: Observations of new aerosol particle formation in a tropical urban atmosphere. Atmos. Environ. 71, 340-351, 2013.

Boulon, J., Sellegri, K., Venzac, H., Picard, D., Weingartner, E., Wehrle, G., Collaud Coen, M., Bütikofer, R., Flückiger, E., Baltensperger, U., Laj, P.: New particle formation and ultrafine charged aerosol climatology at a high-altitude site in the Alps (Jungfraujoch, 3580 m a.s.l., Switzerland). Atmos. Chem. Phys. 10, 9333-9349, 2010.

Boy, M. and Kulmala, M.: Nucleation events in the continental boundary layer: Influence of physical and meteorological parameters. Atmos. Chem. Phys. 2, 1-16, 2002.

Boy, M., Karl, T., Turnipseed, A., Mauldin, R. L., Kosciuch, E., Greenberg, J., Rathbone, J., Smith, J., Held, A., Barsanti, K., Wehner, B., Bauer, S., Wiedensohle, A., Bonn, B., Kulmala, M., Guenther, A.: New particle formation in the Front Range of the Colorado Rocky Mountains, Atmos. Chem. Phys. 8, 1577- 1590, 2008.

Brines, M., Dall'Osto, M., Beddows, D.C.S., Harrison, R.M., Querol, X.: Simplifying aerosol size distributions modes simultaneously detected at four monitoring sites during SAPUSS. Atmos. Chem. Phys. 14, 2973-2986, 2014.

Brines, M., Dall'Osto, M., Beddows, D.C.S., Harrison, R.M., Gómez-Moreno, F., Núñez, L., Artíñano, B., Costabile, F., Gobbi, G.P., Salimi, F., Morawska, L., Sioutas, C., Querol, X.: Traffic and nucleation events as main sources of ultrafine particles in high-insolation developed world cities. Atmos. Chem. Phys. 15, 5929-5945, 2015.

Buonanno, G. and Morawska, L.: Ultrafine particle emission of waste incinerators and comparison to the exposure of urban citizens. Waste Manage. 37, 75-81, 2005.

Carslaw, D. C. and Ropkins, K.: openair - an R package for air quality data analysis. Environmental Modelling & Software. Volume 27-28, 52-61, 2012.

Charron, A. and Harrison, R.M.: Primary particle formation from vehicle emissions during exhaust dilution in the roadside atmosphere, Atmos. Environ. 37, 4109-4119, 2003.

Cheung, H.C., Morawska L., Ristovski Z.D.: Observation of new particle formation in subtropical urban environment. Atmos. Chem. Phys. 11, 3823–3833, 2011.

Coleman, B.K., Lunden, M.M., Destaillats, H., Nazaroff, W.W.: Secondary organic aerosol from ozone-initiated reactions with terpene-rich household products Atmospheric Environment 42, 8234-8245, 2008.

Costabile, F., Birmili, W., Klose, S., Tuch, T., Wehner, B., Wiedensohler, A., Franck, U., König, K., and Sonntag, A.: Spatiotemporal variability and principal components of the particle number size distribution in an urban atmosphere. Atmos. Chem. Phys. 9, 3163-3195, 2009.

Crespí, S.N., Artíñano, B., Cabal, H.: Synoptic classification of the mixed-layer height evolution. Journal of Applied Meteorology, 34, 1668-1677, 1995.

Cusack, M., Pérez, N., Pey, J., Alastuey, A., Querol, X.: Variability of submicrometer particle number size distributions in the western Mediterranean regional background. Tellus B. 65, 19243, doi:10.3402/tellusb.v65i0.19243, 2013a.

Cusack, M., Alastuey, A., Querol, X.: Case studies of new particle formation and evaporation processes in the western Mediterranean regional background. Atmospheric Environment 81, 651-659, 2013b.

Dall'Osto, M., Beddows, D.C.S., Pey, J., Rodriguez, S., Alastuey, A., Harrison, R.M., Querol, X.: Urban aerosol size distributions over the Mediterranean city of Barcelona, NE Spain. Atmos. Chem. Phys. 12, 10693-10707, 2012.

Dall'Osto, M., Querol, X., Alastuey, A., O'Dowd, C., Harrison, R.M., Wenger, J., Gómez-Moreno, F.J.: On the spatial distribution and evolution of ultrafine particles in Barcelona. Atmos. Chem. Phys. 13, 741-759, 2013.

Dal Maso, M., Kulmala, M., Riipinen, I., Wagner, R., Hussein, T., Aalto, P. P., Lehtinen, K. E. J.: Formation and growth of fresh atmospheric aerosols: eight years of aerosol size distribution data from SMEAR II, Hyytiälä, Finland. Boreal Env. Res. 10, 323-336, 2005.

de Gouw, J.A., Goldan, P.D., Warneke, C., Kuster, W.C., Roberts, J.M., Marchewka, M., Bertman, S.B., Pszenny, A.A.P., Keene, W.C: Validation of proton transfer reaction-mass spectrometry (PTR-MS) measurements of gas-phase organic compounds in the atmosphere during the New England air quality study (NEAQS) in 2002, J. Geophys. Res. Atmos. 108 (D21), 2003.

Duncianu, M., David, M., Kartigueyane, S., Cirtog, M., Doussin, J F., Picquet-Varrault, B.: Measurement of alkyl and multifunctional organic nitrates by proton transfer reaction mass spectrometry, Atmospheric Measurement Techniques, 10 (4), 1445-1463, 2017.

El Haddad, I., D'Anna, B., Temime-Roussel, B., Nicolas, M., Boreave, A., Favez, O., Voisin, D., Sciare, J., George, C., Jaffrezo, J.-L., Wortham, H., and Marchand, N.: Towards a better understanding of the origins, chemical composition and aging of oxygenated organic aerosols: case study of a Mediterranean industrialized environment, Marseille, Atmos. Chem. Phys., 13, 7875-7894, doi:10.5194/acp-13-7875-2013, 2013.

García, M.I., Rodríguezs, S., González, Y., García, R.D.: Climatology of new particle formation at Izaña mountain GAW observatory in the subtropical North Atlantic, Atmos. Chem. Phys. 14, 8, 3865-3881, 2014.

Gómez-Moreno, F.J., Pujadas, M., Plaza, J., Rodríguez-Maroto, J.J., Martínez-Lozano, P., Artíñano, B.: Influence of seasonal factors on the atmospheric particle number concentration and size distribution in Madrid, Atmos. Environ. 45, 3199-3180, 2011.

Graus, M., Muller, M., Hansel, A.: High Resolution PTR-TOF: Quantification and Formula Confirmation of VOC in Real Time, Journal of the American Society For Mass Spectrometry, 21, 1037-1044, 2010.

Harrison, R.M., Beddows, D.C.S., Dall'Osto, M.: PMF analysis of wide-range particle size spectra collected on a major highway. Environ. Sci. Technol. 45, 5522-5528, 2011.

Hofman, J., Staelensa, J., Cordell, R., Stroobants, C., Zikova, N., Hama, S.M.L., Wyche, K.P., Kosf, G.P.A., Van Der Zeeg, S., Smallbone, K.L., Weijers, E.P., Monks, P.S.: Ultrafine particles in four European urban environments: Results from a new continuous long-term monitoring network. Atmospheric Environment 136, 68-81, 2016.

Hudda, N., Gould, T., Hartin, K., Larson, T.V., Fruin, S.A.: Emissions from an International Airport Increase Particle Number Concentrations 4-fold at 10 km Downwind. Environ. Sci. Technol., 48 (12), 6628-6635, 2014.

Hussein, T., Dal Maso, M., Petäjä, T., Koponen, I., Paatero, P., Aalto, P., Hämeri, K., Kulmala, M.: Evaluation of an automatic algorithm for fitting the particle number size distributions. Boreal Env. Res., 10, 337-355, 2005.

Hussein, T., Molgaard, B., Hannuniemi, H., Martikainen, J., Järvi, L., Wegner, T., Ripamonti, G., Weber, S., Vesala, T., Hämeri, K.: Fingerprints of the urban particle number size distribution in Helsinki, Finland: Local vs. regional characteristics. Boreal Env. Res. 19, 1-20, 2014.

Hussein, T., Martikainen, J., Junninen, H., Sogacheva, L., Wagner, R., Dal Maso, M., Riipinen, I., Aalto, P. P., Kulmala, M.: Observation of regional new particle formation in the urban atmosphere. Tellus B, 60: 509-521, 2008. doi:10.1111/j.1600-0889.2008.00365.x

Johnson, G.R., Juwono, A.M., Friend, A.J., Cheung, H.-C., Stelcer, E., Cohen, D., Ayoko, G.A., Morawska, L.: Relating urban airborne particle concentrations to shipping using carbon based elemental emission ratios. Atmospheric Environment. 95, 525-536, 2014.

Kecorius, S., Kivekäs, N., Kristenssond, A., Tuch, T., Covert, D.S., Birmili, W. Lihavainen, H., Hyvärinen, A.-P., Martinsson, J., Sporre, M.K., Swietlicki, E., Wiedensohler, A., Ulevicius, V.: Significant increase of aerosol number concentrations in air masses crossing a densely trafficked sea area. Oceanologia 58, 1, 1-12, 2016.

Keuken, M.P., Moerman, M., Zandveld, P., Henzing, J.S., Hoek, G.: Total and size-resolved particle number and black carbon concentrations in urban areas near Schiphol airport (the Netherlands). Atmospheric Environment 104, 132-142, 2015.

Kirkby, J., Duplissy, J., Sengupta, K., Frege, C., Gordon, H., Williamson, C., Heinritzi, M., Simon, M., Yan, C., Almeida, J., Trostl, J., Nieminen, T., Ortega, I.K., Wagner, R., Adamov, A., Amorim, A., Bernhammer, A.K., Bianchi, F., Breitenlechner, M., Brilke, S., Chen, X., Craven, J., Dias, A., Ehrhart, S., Flagan, R.C., Franchin, A., Fuchs, C., Guida, R., Hakala, J., Hoyle, C.R., Jokinen, T., Junninen, H., Kangasluoma, J., Kim, J., Krapf, M., Kurten, A., Laaksonen, A., Lehtipalo, K., Makhmutov, V., Mathot, S., Molteni, U., Onnela, A., Perakyla, O., Piel, F., Petaja, T., Praplan, A.P., Pringle, K., Rap, A., Richards, N.A.D., Riipinen, I., Rissanen, M.P., Rondo, L., Sarnela, N., Schobesberger, S., Scott, C.E., Seinfeld, J.H., Sipila, M., Steiner, G., Stozhkov, Y., Stratmann, F., Tomé, A., Virtanen, A., Vogel, A.L., Wagner, A.C., Wagner, P.E., Weingartner, E., Wimmer, D., Winkler, P.M., Ye, P., Zhang, X., Hansel, A., Dommen, J., Donahue, N.M., Worsnop, D.R., Baltensperger, U., Kulmala, M., Carslaw, K.S., Curtius, J.: Ion-induced nucleation of pure biogenic particles. Nature 533, 521–526, doi:10.1038/nature17953, 2016.

Kittelson, D.B., Watts, W.F., Johnson, J.P.: On-road and laboratory evaluation of combustion aerosols – Part1: Summary of diesel engine results. J. Aerosol Sci. 37, 913-930, 2006.

Kontkanen, J., Lehtipalo, K., Ahonen, L., Kangasluoma, J., Manninen, H.E., Hakala, J., Rose, C., Sellegri, K., Xiao, S., Wang, L., Qi, X., Nie, W., Ding, A., Yu, H., Lee, S., Kerminen, V.-M., Petäjä, T., Kulmala, M.: Measurements of sub-3 nm particles using a particle size magnifier in different environments: from clean mountain top to polluted megacities. Atmos. Chem. Phys., 17, 2163-2187, 2017.

Kulmala, M., Pirjola, L., Mäkelä, J.M.: Stable Sulphate Clusters as a Source of New Atmospheric Particles, Nature, 404, 66-69, 2000.

Kulmala, M., Vehkamehk, H., Pet, P.T., Dal Maso, M., Lauri, A., Kerminen, V.-M., Birmili, W., McMurry, P.: Formation and growth rates of ultrafine atmospheric particles: a review of observations. J. Aerosol Sci. 35, 143-176, 2004.

Kulmala, M. and Kerminen, V.-M.: On the formation and growth of atmospheric nanoparticles, Atmos. Research 90, 132-150, 2008.

Kulmala, M., Petäjä, T., Nieminen, T., Sipilä, M., Manninen, H. E., Lehtipalo, K., Dal Maso, M., Aalto, P. P., Junninen, H., Paasonen, P., Riipinen, I., Lehtinen, K. E. J., Laaksonen, A., Kerminen, V-M.: Measurement of the nucleation of atmospheric aerosol particles. Nature Protocols, 7, 1651-1667, 2012.

Kulmala, M., Luoma, K., Virkkula, A., Petäjä, T., Paasonen, P., Kerminen, V.M., Nie, W., Qi, X., Shen, Y., Chi, X., Ding, A.: On the mode-segregated aerosol particle number concentration load: Contributions of primary and secondary particles in Hyytiälä and Nanjing. Boreal Environ. Res. 21, 319–331, 2016.

Kumar, P. and Morawska, L.: Recycling Concrete: An Undiscovered Source of Ultrafine Particles. Atmos. Environ 90, 51-58, 2014.

Kumar, P., Morawska, L., Birmili, W., Paasonen, P., Hu, M., Kulmala, M., Harrison, R.M., Norford, L., Britter, R.: Ultrafine particles in cities, Environ. Int. 66, 1-10, 2014.

Lee, H.-K., Hwang, I.-K., Ahn, K.-H.: Development and Evaluation of Hy-CPC. Particle and Aerosol Research 10, 93-97, 2014.

Lee, H.-K., Eun, H.-R., Lee, G.-H., Ahn, K.-H.: Development and evaluation of Hy-SMPS, Particle and Aerosol Research 11, 57-61, 2015.

~~Liu, Z.R., Hu, B., Liu, Q., Sun, Y., Wang, Y.S.: Source apportionment of urban fine particle number concentration during summertime in Beijing. Atmos. Environ. 95, 359-369, 2014.~~

Ma, N. and Birmili, W.: Estimating the contribution of photochemical particle formation to ultrafine particle number averages in an urban atmosphere. Science of the Total Environment 512–513, 154-166, 2015.

Manninen, H. E., Nieminen, T., Asmi, E., Gagné, S., Häkkinen, S., Lehtipalo, K., Aalto, P., Vana, M., Mirme, A., Mirme, S., Hõrrak, U., Plass-Dülmer, C., Stange, G., Kiss, G., Hoffer, A., Töro, N., Moerman, M., Henzing, B., De Leeuw, G., Brinkenberg, M., Kouvarakis, G. N., Bougiatioti, A., Mihalopoulos, N., O'Dowd, C., Ceburnis, D., Arneth, A., Svenningsson, B., Swietlicki, E., Tarozzi, L., Decesari, S., Facchini, M. C., Birmili, W., Sonntag, A., Wiedensohler, A., Boulon, J., Sellegri, K., Laj, P., Gysel, M., Bukowiecki, N., Weingartner, E., Wehrle, G., Laaksonen, A., Hamed, A., Joutsensaari, J., Petäjä, T., Kerminen, V. M. and Kulmala, M.: EUCAARI ion spectrometer measurements at 12 European sites-analysis of new particle formation events, Atmos. Chem. Phys., 10(16), 7907–7927, doi:10.5194/acp-10-7907-2010, 2010.

Masiol, M., Harrison, R. M., Vu, T. V., Beddows, D. C. S.: Sources of sub-micrometre particles near a major international airport, Atmos. Chem. Phys., 17, 12379-12403, doi:10.5194/acp-17-12379-2017, 2017.

~~Mazaheri, M., Johnson, G. R., Morawska, L.: Particle and gaseous emissions from commercial aircraft at each stage of the landing and takeoff cycle. Environmental Science and Technology, 43, 441-446, 2009.~~

Minguillón, M.C., Brines, M., Pérez, N., Reche, C., Pandolfi, M., Fonseca, A.S., Amato, F., Alastuey, A., Lyasota, A., Codina, B., Lee, H.-K., Eun, H.-R., Ahn, K.-H., Querol, X.: New particle formation at ground level and in the vertical column over the Barcelona area. Atmospheric Research 164–165, 118–130, 2015.

Nie, W., Ding, A., Wang, T., Kerminen, V.M., George, C., Xue, L., Wang, W., Zhang, Q., Petäjä, T., Qi, X., Gao, X., Wang, X., Yang, X., Fu, C., Kulmala, M.: Erratum: Polluted dust promotes new particle formation and growth, Sci. Rep., doi:10.1038/srep08949, 2015.

O'Dowd, C., Monahan, C., Dall'Osto, M.: On the occurrence of open ocean particle production and growth events, Geophys. Res. Lett., 37, L19805, doi:10.1029/2010GL044679, 2010.

Paasonen, P., Kupiainen, K., Klimont, Z., Visschedijk, A., Denier van der Gon, H. A. C., and Amann, M.: Continental anthropogenic primary particle number emissions, Atmos. Chem. Phys., 16, 6823-6840, doi:10.5194/acp-16-6823-2016, 2016.

Park, J.H., Goldstein, A.H., Timkovsky, J., Fares, S., Weber, R., Karlik, J., Holzinger, R.: Active atmosphere–ecosystem exchange of the vast majority of detected volatile organic compounds. Science, 341, 643–647, 2013.

Pey, J., Rodríguez, S., Querol, X., Alastuey, A., Moreno, T., Putaud, J.P., Van Dingenen, R.: Variations of urban aerosols in the western Mediterranean. Atmos. Environ. 42, 9052-9062, 2008.

Pey, J., Querol, X., Alastuey, A., Rodríguez, S., Putaud, J. P., Van Dingenen, R.: Source Apportionment of urban fine and ultrafine particle number concentration in a Western Mediterranean city. Atmos. Environ. 43, 4407-4415, 2009.

Plaza, J., Pujadas, M., Artíñano, B.: Formation and Transport of the Madrid Ozone Plume. J. Air & Waste Manage. Assoc. 47, 766-774, 1997.

Qian, S., Sakurai, H., McMurry, P.H.: Characteristics of regional nucleation events in urban East St. Louis. Atmospheric Environment, 41, 4119-4127, 2007.

Querol, X., Gangoiti, G., Mantilla, E., Alastuey, A., Minguillón, M. C., Amato, F., Reche, C., Viana, M., Moreno, T., Karanasiou, A., Rivas, I., Pérez, N., Ripoll, A., Brines, M., Ealo, M., Pandolfi, M., Lee, H.-K., Eun, H.-R., Park, Y.-H., Escudero, M., Beddows, D., Harrison, R.M., Bertrand, A., Marchand, N., Lyasota, A., Codina, B., Olid, M., Udina, M., Jiménez-Esteve, B., Soler, M.R., Alonso, L., Millán, M., Ahn, K.-H.: Phenomenology of high-ozone episodes in NE Spain. Atmos. Chem. Phys. 17, 2817-2838, 2017~~a~~.

Querol, X., Alastuey, A., Gangoiti, G., Perez, N., Lee, H. K., Eun, H. R., Park, Y., Mantilla, E., Escudero, M., Titos, G., Alonso, L., Temime-Roussel, B., Marchand, N., Moreta, J. R., Revuelta, M. A., Salvador, P., Artíñano, B., García dos Santos, S., Anguas, M., Notario, A., Saiz-Lopez, A., Harrison, R. M., Millán, M., and Ahn, K.-H.: Phenomenology of summer ozone episodes over the Madrid Metropolitan Area, central Spain, Atmos. Chem. Phys., 18, 6511-6533, https://doi.org/10.5194/acp-18-6511-2018, 2018.~~Querol, X., Alastuey, A., Gangoiti, G., Perez, N., Lee, H. K., Eun, H. R., Park, Y., Mantilla, E., Escudero, M., Titos, G., Alonso, L., Temime-Roussel, B., Marchand, N., Moreta, J. R., Revuelta, M. A., Salvador, P., Artíñano, B., García dos Santos, S., Anguas, M., Notario, A., Saiz-Lopez, A., Harrison, R. M., and Ahn, K.-H.: Phenomenology of summer ozone episodes over the Madrid Metropolitan Area, central Spain, Atmos. Chem. Phys. Discuss., doi:10.5194/acp-2017-1014, in review, 2017b.~~

Reche, C., Querol, X., Alastuey, A., Viana, M., Pey, J., Moreno, T., Rodríguez, S., González, Y., Fernández-Camacho, R., de la Rosa, J., Dall'Osto, M., Prévôt, A.S.H., Hueglin, C., Harrison, R.M., Quincey, P.: New considerations for PM, Black Carbon and particle number concentration for air quality monitoring across different European cities. Atmos. Chem. Phys. 11, 6207-6227, 2011.

~~Rimnácová, D., Zdímal, V., Schwarz, J., Smolík, J., Rimnác, M.: Atmospheric aerosols in suburb of Prague: The dynamics of particle size distributions. Atmos. Res. 101, 539-552, 2011.~~

Roberts, J. M.: Measurement of the Henry's law coefficient and first order loss rate of PAN in n-octanol, Geophys. Res. Lett., 32, L08803, doi:10.1029/2004gl022327, 2005.

Robinson, A.L., Donahue, N.M., Shrivastava, M.K., Weitkamp, E.A., Sage, A.M., Grieshop, A.P., Lane, T.E., Pierce, J.R., Pandis, S.N.: Rethinking organic aerosols: semivolatile emissions and photochemical aging. Science 31, 1259-1262, 2007.

Rönkkö, T., Kuuluvainen, H., Karjalainen, P., Keskinen, J., Hillamo, R., Niemi, J. V, Pirjola, L., Timonen, H.J., Saarikoski, S., Saukko, E., Järvinen, A., Silvennoinen, H., Rostedt, A., Olin, M., Yli-Ojanperä, J., Nousiainen, P., Kousa, A., Dal Maso, M.: Traffic is a major source of atmospheric nanocluster aerosol. Proc. Natl. Acad. Sci. U. S. A. 114, 7549–7554, doi:10.1073/pnas.1700830114, 2017.

Saiz-Lopez, A., Borge, R., Notario, A., Adame, J.A., De la Paz, D., Querol, X., Artíñano, B., Gomez-Moreno, F.J., Cuevas, C.A.: Unexpected increase in the oxidation capacity of the urban atmosphere of Madrid, Spain, Sci. Rep., 7, 45956, doi:10.1038/srep45956, 2017.

Salimi, F., Ristovski, Z., Mazaheri, M., Laiman, R., Crilley, L. R., He, C., Clifford, S., and Morawska, L.: Assessment and application of clustering techniques to atmospheric particle number size distribution for the purpose of source apportionment. Atmos. Chem. Phys. 14, 11883-11892, 2014.

Salma, I., Borsós, T., Weidinger, T., Aalto, P., Hussein, T., Dal Maso, M., Kulmala, M.: Production, growth and properties of ultrafine atmospheric aerosol particles in an urban environment. Atmos. Chem. Phys. 11, 1339-1353, 2011.

Salma, I., Borsos T., Nemeth Z., Weidiger T., Aalto P., Kulmala M.: Comparative study of ultrafine atmospheric aerosol within a city. Atmos. Environ., 92, 154-161, 2014.

Salma, I., Németh, Z., Kerminen, V-M., Aalto, P., Nieminen, T., Weidinger, T., Molnár, Á., Imre, K., Kulmala, M.: Regional effect on urban atmospheric nucleation, Atmospheric Chemistry and Physics 16, 8715-8728, 2016.

Salvador, P., Artíñano, B., Viana, M., Alastuey, A., Querol, X.: Multicriteria approach to interpret the variability of the levels of particulate matter and gaseous pollutants in the Madrid metropolitan area, during the 1999-2012 period. Atmospheric Environment 109, 205-216, 2015.

Sellegri, K., Laj, P., Venzac, H., Boulon, J., Picard, D., Villani, P., Bonasoni, P., Marinoni, A., Cristofanelli, P., Vuillermoz, E.: Seasonal variations of aerosol size distributions based on longterm measurements at the high altitude Himalayan site of Nepal Climate Observatory-Pyramid (5079 m), Nepal. Atmos. Chem. Phys. 10, 10679-10690, 2010.

Sipila, M., Berndt, T., Petaja, T., Brus, D., Vanhanen, J., Stratmann, F., Patokoski, J., Mauldin, R. L., Hyvärinen, A. P., Lihavainen, H. and Kulmala, M.: The role of sulfuric acid in atmospheric nucleation, Science, 327(5970), 1243–1246, doi:10.1126/science.1180315, 2010.

Shi, J.P. and Harrison, R.M.: Investigation of ultrafine particle formation during diesel exhaust dilution. Environ. Sci. Technol. 33, 3730-3736, 1999.

Shi, J.P., Mark, D., Harrison, R.M.: Characterization of particles from a current technology heavy-duty diesel engine, Environ. Sci. Technol., 34, 748-755, 2000.

Skrabalova, L., Zikova, N., Zdimal, V.: Shrinkage of newly formed particles in an urban environment. Aerosol Air Qual. Res. 15, 1313-1324, 2015.

Stanier, C.O., Khlystov, A.Y., Pandis, S.N.: Ambient aerosol size distributions and number concentrations measured during the Pittsburgh Air Quality Study (PAQS). Atmos. Environ., 38, 3275-3284, 2004.

Stolzenburg, M.R., McMurry, P.H., Sakurai, H., Smith, J.N., Lee, M.R., Eisele, F.L., Clement, C.F.: Growth rates of freshly nucleated atmospheric particles in Atlanta. Journal of Geophysical Research, 110, D22S05, 2005.

Stratmann, F., Siebert, H., Spindler, G., Wehner, B., Althausen, D., Heintzenberg, J., Hellmuth, O., Rinke, R., Schmieder, U., Seidel, C., Tuch, T., Uhrner, U., Wiedensohler, A., Wandinger, U., Wendisch, M., Schell, D., and Stohl, A.: New-particle formation events in a continental boundary layer: first results from the SATURN experiment, Atmos. Chem. Phys., 3, 1445-1459, doi:10.5194/acp-3-1445-2003, 2003.

Tröstl, J., Chuang, W. K., Gordon, H., Heinritzi, M., Yan, C., Molteni, U., Ahlm, L., Frege, C., Bianchi, F., Wagner, R., Simon, M., Lehtipalo, K., Williamson, C., Craven, J. S., Duplissy, J., Adamov, A., Almeida, J., Bernhammer, A. K., Breitenlechner, M., Brilke, S., Dias, A., Ehrhart, S., Flagan, R. C., Franchin, A., Fuchs, C., Guida, R., Gysel, M., Hansel, A., Hoyle, C. R., Jokinen, T., Junninen, H., Kangasluoma, J., Keskinen, H., Kim, J., Krapf, M., Kürten, A., Laaksonen, A., Lawler, M., Leiminger, M., Mathot, S., Möhler, O., Nieminen, T., Onnela, A., Petäjä, T., Piel, F. M., Miettinen, P., Rissanen, M. P., Rondo, L., Sarnela, N., Schobesberger, S., Sengupta, K., Sipilä, M., Smith, J. N., Steiner, G., Tomè, A., Virtanen, A., Wagner, A. C., Weingartner, E., Wimmer, D., Winkler, P. M., Ye, P., Carslaw, K. S., Curtius, J., Dommen, J., Kirkby, J.,

Kulmala, M., Riipinen, I., Worsnop, D. R., Donahue, N. M. and Baltensperger, U.: The role of low-volatility organic compounds in initial particle growth in the atmosphere, Nature, 533(7604), 527–531, doi:10.1038/nature18271, 2016.

Stull, R.B.: An introduction to boundary layer meteorology. Kluwer Academic Publishers, Dordrecht, Boston and London, 1988.

United Nations, Department of Economic and Social Affairs: World Urbanization Prospects (2007 revision). https://www.un.org/esa/population/publications/wup2007/2007WUP_Highlights_web.pdf, 2008.

Uhrner, U., von Lowis, S., Vehkamaki, H., Wehner, B., Brasel, S., Hermann, M., Stratmann, F., Kulmala, M., Wiedensohler, A.: Dilution and aerosol dynamics within a diesel car exhaust plume – CFD simulations of on-road conditions. Atmos. Environ. 41, 7440-7461, 2007.

Vakkari, V., Laakso, H., Kulmala, M., Laaksonen, A., Mabaso, D., Molefe, M., Kgabi, N., Laakso, L.: New particle formation events in semi-clean South African Savannah. Atmos. Chem. Phys. 11, 3333-3346, 2011.

von Bismarck-Osten, C., Birmili, W., Ketzel, M., Massling, A., Petäjä, T., Weber, S.: Characterization of parameters influencing the spatio-temporal variability of urban particle number size distributions in four European cities. Atmos. Environ. 77, 415-429, 2013.

Wang, N., Sun, X., Chen, J., Li, X.: Sci. Heterogeneous Nucleation of Trichloroethylene Ozonation Products in the Formation of New Fine Particles. Rep., 7: 42600, doi:10.1038/srep42600, 2017.

Wegner, T., Hussein, T., Hämeri, K, Vesala, T., Kulmala, M., Weber, S.: Properties of aerosol signature size distributions in the urban environment as derived by cluster analysis. Atmos. Environ. 61, 350-360, 2012.

Wehner, B. and Wiedensohler, A.: Long term measurements of submicrometer urban aerosols: statistical analysis for correlations with meteorological conditions and trace gases, Atmos. Chem. Phys., 3, 867-879, https://doi.org/10.5194/acp-3-867-2003, 2003.

Wehner, B., Siebert, H., Stratmann, F., Tuch, T., Wiedensohler, A., Petäjä, T., Dal Maso, M., Kulmala, M.: Horizontal homogeneity and vertical extent of new particle formation events. Tellus 59B, 362-371, 2007.

Wehner, B., Siebert, H., Ansmann, A., Ditas, F., Seifert, P., Stratmann, F., Wiedensohler, A., Apituley, A., Shaw, R. A., Manninen, H. E., and Kulmala, M.: Observations of turbulence-induced new particle formation in the residual layer, Atmos. Chem. Phys., 10, 4319-4330, doi:10.5194/acp-10-4319-2010, 2010.

Wiedensohler, A., Wehner, B., Birmili, W.: Aerosol number concentrations and size distributions at mountain-rural, urbaninfluenced rural, and urban-background sites in Germany. J. Aerosol Med. 15, 237-243, 2002.

Woo, K.S., Chen, D.R., Pui, D.Y.H., McMurry, P.H.: Measurement of Atlanta aerosol size distributions: observations of ultrafine particle events. Aerosol Sci. Tech. 34, 75-87, 2001.

~~Wu, Z., Hu, M., Liu, S., Wehner, B., Wiedensohler, A.: Particle number size distribution in the urban atmosphere of Beijing, China. Atmos. Environ. 42, 7967-7980, 2008.~~

Yao, X., Choi, M.Y., Lau, N.T., Lau, A.P.S., Chan, C.K., Fang, M.: Growth and shrinkage of new particles in the atmosphere in Hong Kong. Aerosol Sci. Tech. 44, 639-650, 2010.

Young, L.-H., Lee, S.-H., Kanawade, V.P., Hsiao, T.-C., Lee, Y.L., Hwang, B.-F., Liou, Y.-J., Hsu, H.-T., Tsai, P.-J.: New particle growth and shrinkage observed in subtropical environments, Atmos. Chem. Phys. 13, 547-564, 2013.

**Table 1: Summary of new particle formation events recorded during the campaign showing the starting time, considered as the moment of first detection of the nucleation mode, the final time, considered when the mode reaches 25 nm, ~~and~~ the growth rate calculated in that period using SMPS and PSM data, and formation rates at starting time. A star marks the events that are detected simultaneously at all stations and were chosen for further analysis in this work.**

| | Date | Starting Time (UTC) | Final Time (UTC) | GR (nm $h^{-1}$) | $GR_{PSM}$ (nm $h^{-1}$) | $J_1$ ($cm^{-3}$ $s^{-1}$) |
|---|---|---|---|---|---|---|
| CSIC | 12/07/2016 (*) | 6:20 | 10:39 | 3.9 | 1.9 | 2.4 |
| | 13/07/2016 (*) | 8:30 | 12:49 | 2.0 | 1.1 | 8.5 |
| | 14/07/2016 (*) | 8:45 | 11:53 | 1.4 | 6.75 | 15.7 |
| ISCIII | 12/07/2016 (*) | 5:30 | 9:44 | 3.0 | 0.7 | 1.9 |
| | 13/07/2016 (*) | 8:50 | 11:54 | 4.6 | 4.3 | 8.1 |
| | 14/07/2016 (*) | 9:20 | 10:39 | 5.4 | 6.8 | 6.5 |
| | 16/07/2016 (*) | 11:30 | 13:14 | 10.0 | 4.3 | - |
| | 17/07/2016 (*) | 8:25 | 10:20 | 7.1 | 4.4 | 3.2 |
| | 18/07/2016 (*) | 10:44 | 12:20 | 2.9 | 1.38 | 6.8 |
| CIEMAT | 13/07/2016 (*) | 8:15 | 13:45 | 2.5 | - | - |
| | 14/07/2016 (*) | 9:00 | 13:10 | 4.1 | - | - |
| | 15/07/2016 | 8:34 | 13:08 | 4.0 | - | - |
| | 16/07/2016 (*) | 9:40 | 13:03 | 2.8 | - | - |
| | 17/07/2016 (*) | 9:55 | 13:00 | 2.8 | - | - |
| | 18/07/2016 (*) | 9:09 | 11:49 | 2.6 | - | - |
| MJDH -Sounding | 12/07/2016 | 7:27 | 8:08 | 3.5 | - | - |
| | 13/07/2016 | 8:39 | 9:56 | 5.3 | - | - |
| | 14/07/2016 | 9:00 | 10:34 | 6.2 | - | - |

## Figure captions

Figure 1: Particle size distribution at CSIC, CIEMAT and ISCIII from 4 to 20 July 2016. Total particle concentration of particles with diameter greater than 2.5 nm is also shown.~~Particle size distribution of the regional new particle formation episodes detected during the intensive field campaign (a) at CSIC (up) and ISCIII (down) in 12-14 July, and (b) at CIEMAT (up) and ISCIII (down) in 16-18 July. For CIEMAT data only the long SMPS is represented here.~~

Figure 2: Boxplot of growth rates (GR) determined for the nucleation mode (< 25 nm) during regional new particle formation events at urban (CSIC or CIEMAT) and suburban (ISCIII) stations. The red line represents the median, the upper and lower limits of the boxes represent the 75th and 25th percentiles and the whiskers include 99.3% of the data. Outliers are represented with a red cross.

Figure 3: Averaged daily cycles of (a) total particle concentration in the size range 9-25 nm, (b) total concentration of particles >2.5 nm measured with PSM at CSIC and ISCIII (c) Condensation Sink (CS) and (d) Coagulation Sink (CoagS) during regional new particle formation events at urban (CSIC and CIEMAT, solid line) and suburban (ISCIII, dashed line) stations. The hour of the day is UTC. Local time is UTC+2.

Figure 4: Particle size distribution with fitted log-normal modes (black dots) measured during the balloons soundings at Majadahonda on 12 July 2016. An estimation of the mixing layer height is represented with red dots. The altitude of the instrumentation is represented with a white line. Surface level is 630 m above sea level. Time is UTC. Local time is UTC+2.

Figure 5: Particle size distribution with fitted log-normal modes (black dots) measured during the balloons soundings at Majadahonda on 13 July 2016. The altitude of the instrumentation is represented with a white line. Surface level is 630 m above sea level. Time is UTC. Local time is UTC+2.

Figure 6: Particle size distribution with fitted log-normal modes (black dots) measured during the balloons soundings at Majadahonda on 14 July 2016. The altitude of the instrumentation is represented with a white line. An estimation of the mixing layer height is represented with red dots. Surface level is 630 m above sea level. Time is UTC. Local time is UTC+2.

Figure 7: Vertical particle size distribution measured on 14 July during selected soundings.

Figure ~~2~~8:~~–~~ Boxplot of shrinkage rate (SR) determined during regional NPF events at urban (CSIC and CIEMAT) and suburban (ISCIII) stations according to the starting diameter of the shrinking particles. The considered categories are~~:~~

particles with a starting diameter below 40 nm and, particles with a starting diameter between 40 and 100 nm, and particles with a starting diameter larger than 100 nm (Acc). The red line represents the median, the upper and lower limits of the boxes represent the 75th and 25th percentiles and the whiskers include 99.3% of the data. Outliers are represented with a red cross.

Figure 3: Bipolar plot of (a) total particle concentration in the size range 1.2-4 nm measured with the PSM, (b) Black Carbon, (c) $NO_2$ and (d) NO concentrations at CSIC urban station, using the wind data registered at CIEMAT. Daylight and nighttime hours are separated according to sunrise (5 UTC) and sunset (20 UTC) hours. The data correspond to the period 11-15 July 2016.

Figure 4: Boxplot of growth rates (GR) determined for the nucleation mode (< 25 nm) during regional new particle formation events at urban (CSIC or CIEMAT) and suburban (ISCIII) stations. The red line represents the median, the upper and lower limits of the boxes represent the 75th and 25th percentiles and the whiskers include 99.3% of the data. Outliers are represented with a red cross.

Figure 5: Averaged daily cycles of (a) total particle concentration in the size range 9-25 nm, (b) Condensation Sink (CS) and (c) Coagulation Sink ($CoagS_9$) during regional new particle formation events at urban (CSIC and CIEMAT, solid line) and suburban (ISCIII, dashed line) stations. The hour of the day is UTC. Local time is UTC+2.

Figure 6: Hourly formation rates in the ranges 9.1-25 nm at (a) urban (CSIC or CIEMAT) and (b) suburban (ISCIII) stations during regional new particle formation events. The red line represents the median, the upper and lower limits of the boxes represent the 75th and 25th percentiles and the whiskers represent the 5th and 95th percentiles. Time is UTC. Local time is UTC+2.

Figure 9: Bipolar plot of (a) total particle concentration in the size range 1.2-4 nm measured with the PSM, (b) Black Carbon, (c) $NO_2$ and (d) NO concentrations at CSIC urban station, using the wind data registered at CIEMAT. Daylight and nighttime hours are separated according to sunrise (5 UTC) and sunset (20 UTC) hours. The data correspond to the period 11-15 July 2016.

Figure 7: Particle size distribution with fitted log-normal modes measured during the balloons soundings at Majadahonda on 12 July 2016. The altitude of the instrumentation is represented with a white line. Surface level is 630 m above sea level. Time is UTC. Local time is UTC+2.

Figure 8: Particle size distribution with fitted log-normal modes measured during the balloons soundings at Majadahonda on 13 July 2016. The altitude of the instrumentation is represented with a white line. Surface level is 630 m above sea level. Time is UTC. Local time is UTC+2.

Figure 9: Particle size distribution with fitted log-normal modes measured during the balloons soundings at Majadahonda on 14 July 2016. The altitude of the instrumentation is represented with a white line. Surface level is 630 m above sea level. Time is UTC. Local time is UTC+2.

Figure 10: Vertical particle size distribution measured on 14 July during selected soundings.

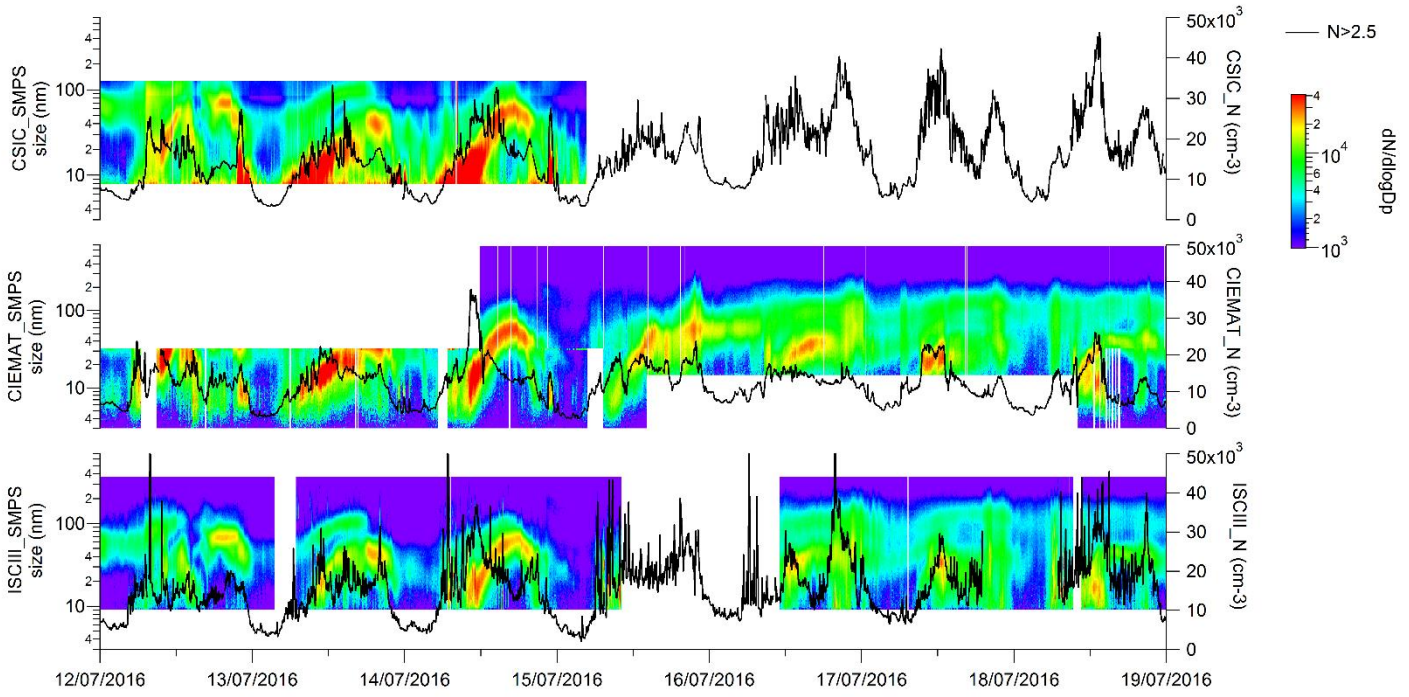


Figure 1

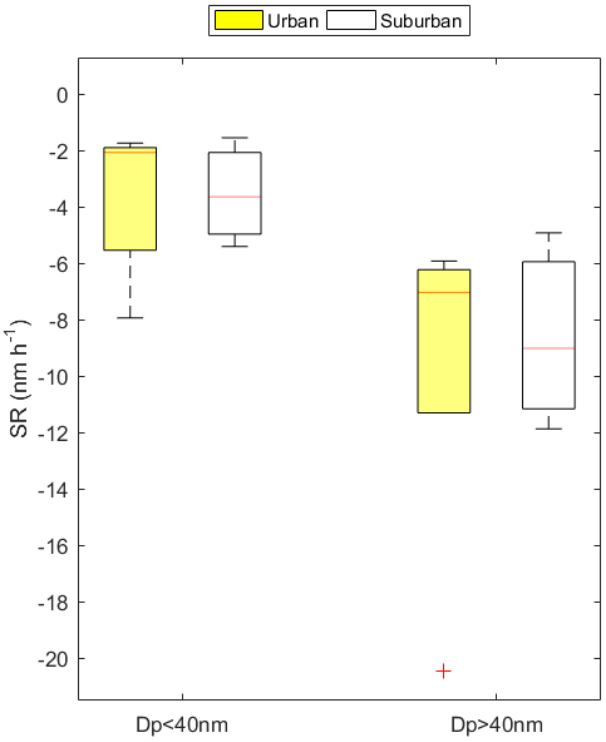


~~Figure 2~~

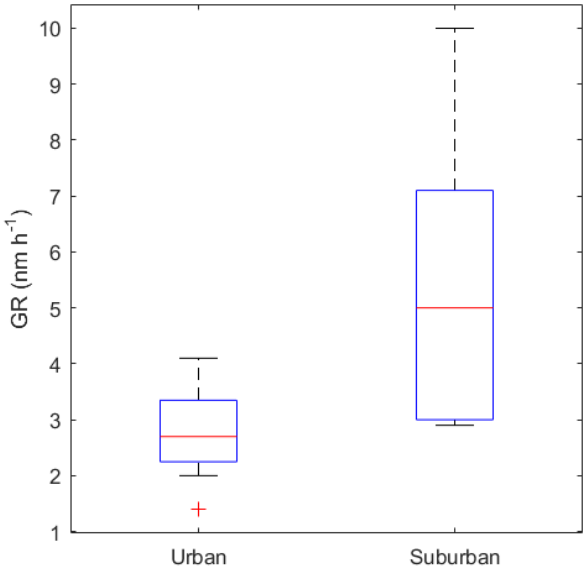


Figure 23

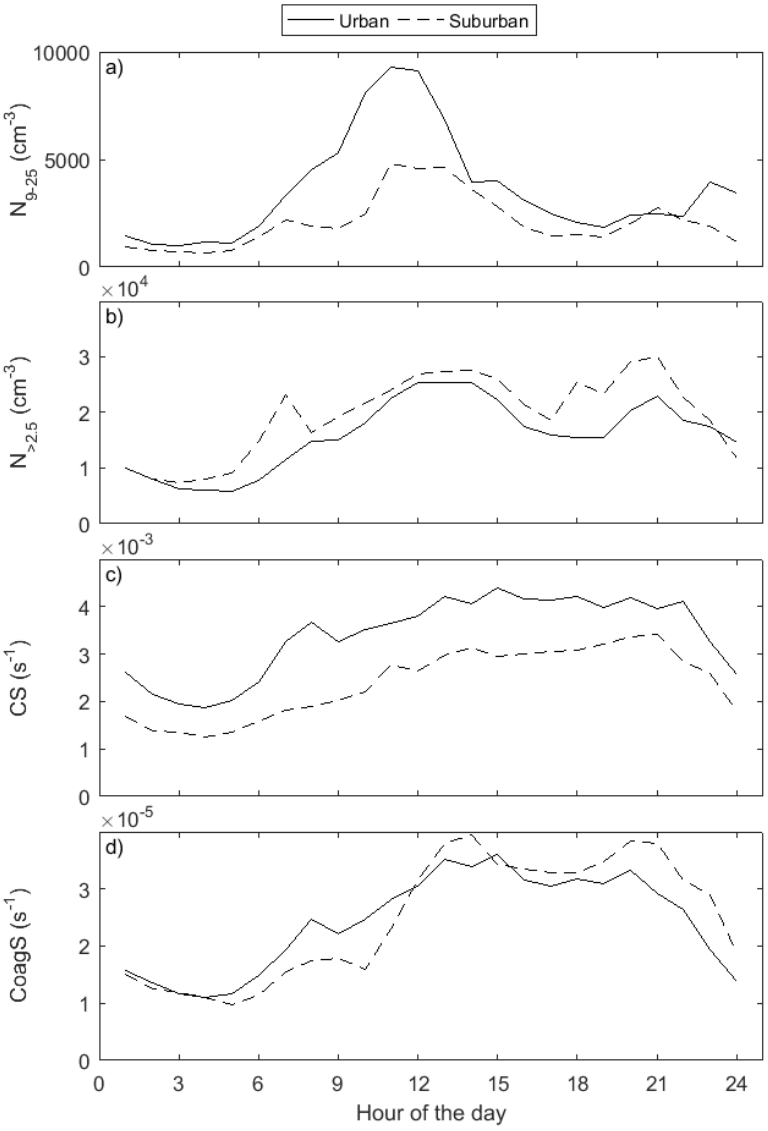


Figure 34

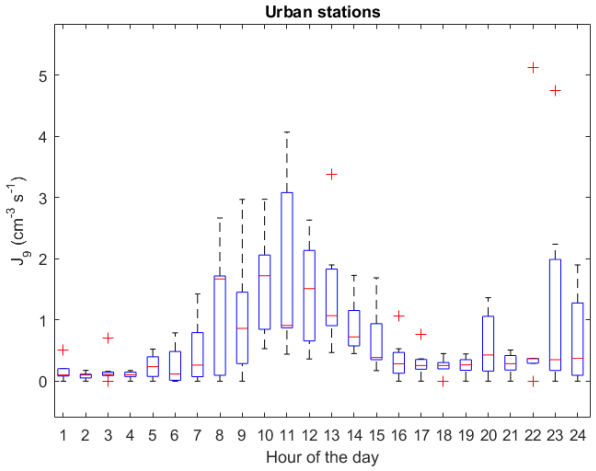


~~Figure 5a~~

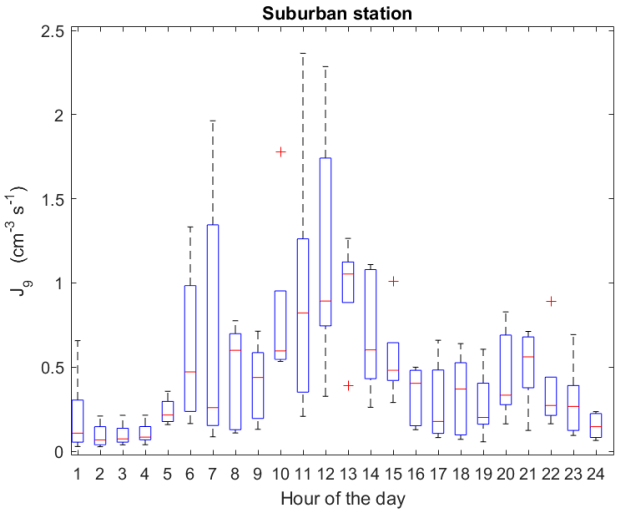


~~Figure 5b~~

5

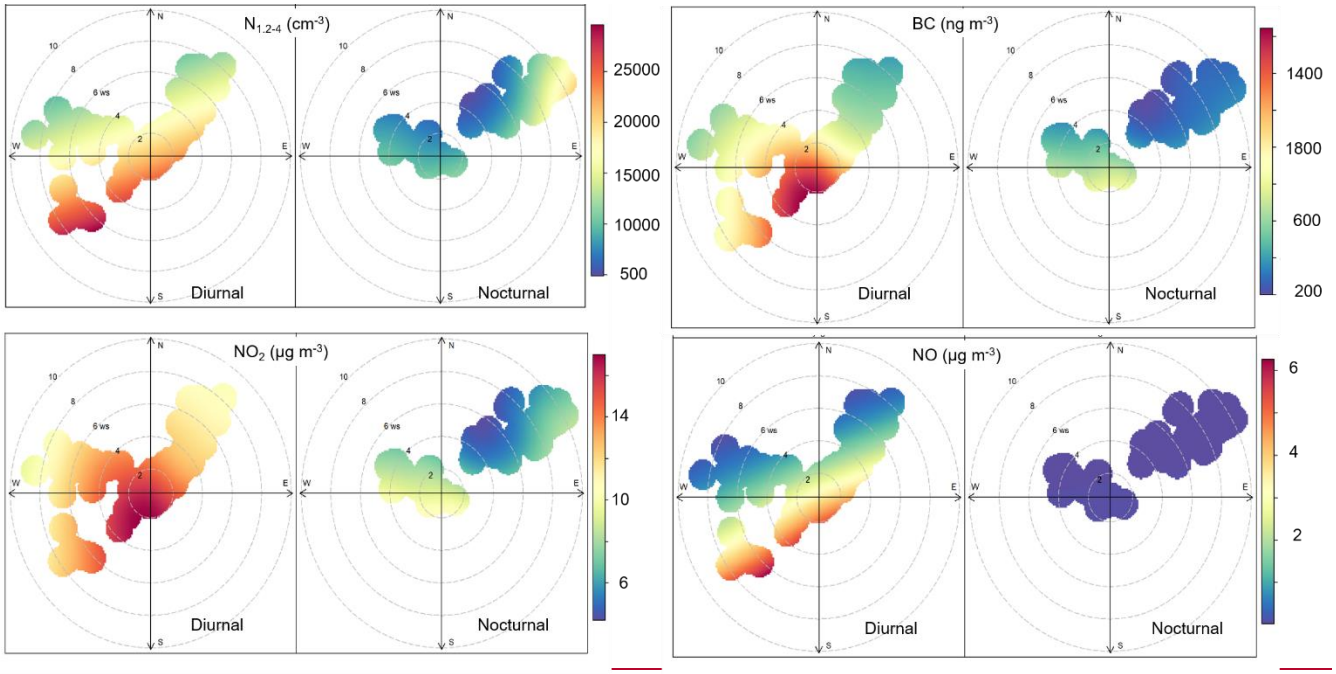
N1.2-4 (cm-3)
BC (ng m-3)
NO2 (µg m-3)
NO (µg m-3)
Diurnal
Nocturnal
25000
20000
15000
10000
500
1400
1800
600
200
14
10
6
6
4
2

~~Figure 6~~

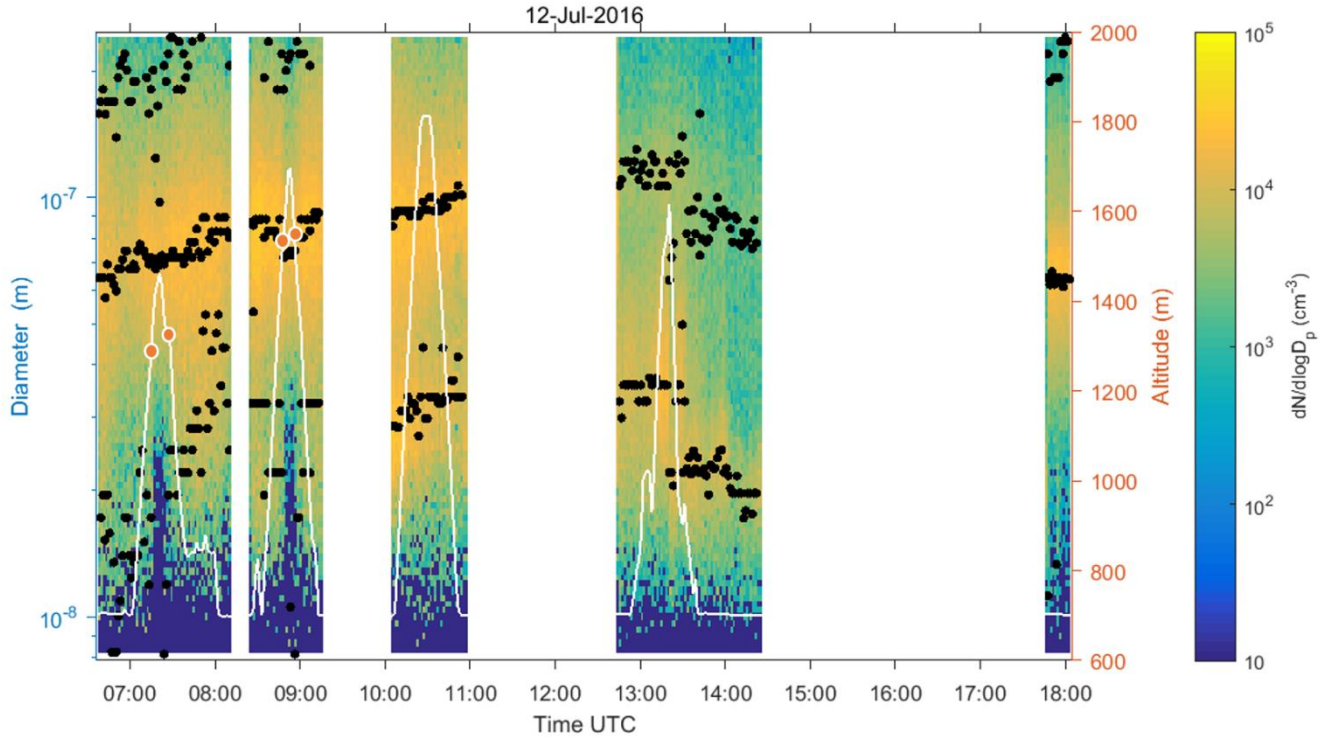
12-Jul-2016
Diameter (m)
10-7
10-8
Altitude (m)
2000
1800
1600
1400
1200
1000
800
600
dN/dlogDp (cm-3)
10^5
10^4
10^3
10^2
10
07:00
08:00
09:00
10:00
11:00
12:00
13:00
14:00
15:00
16:00
17:00
18:00
Time UTC

Figure ~~47~~

Figure 5

~~Figure 8~~

~~Figure 9~~

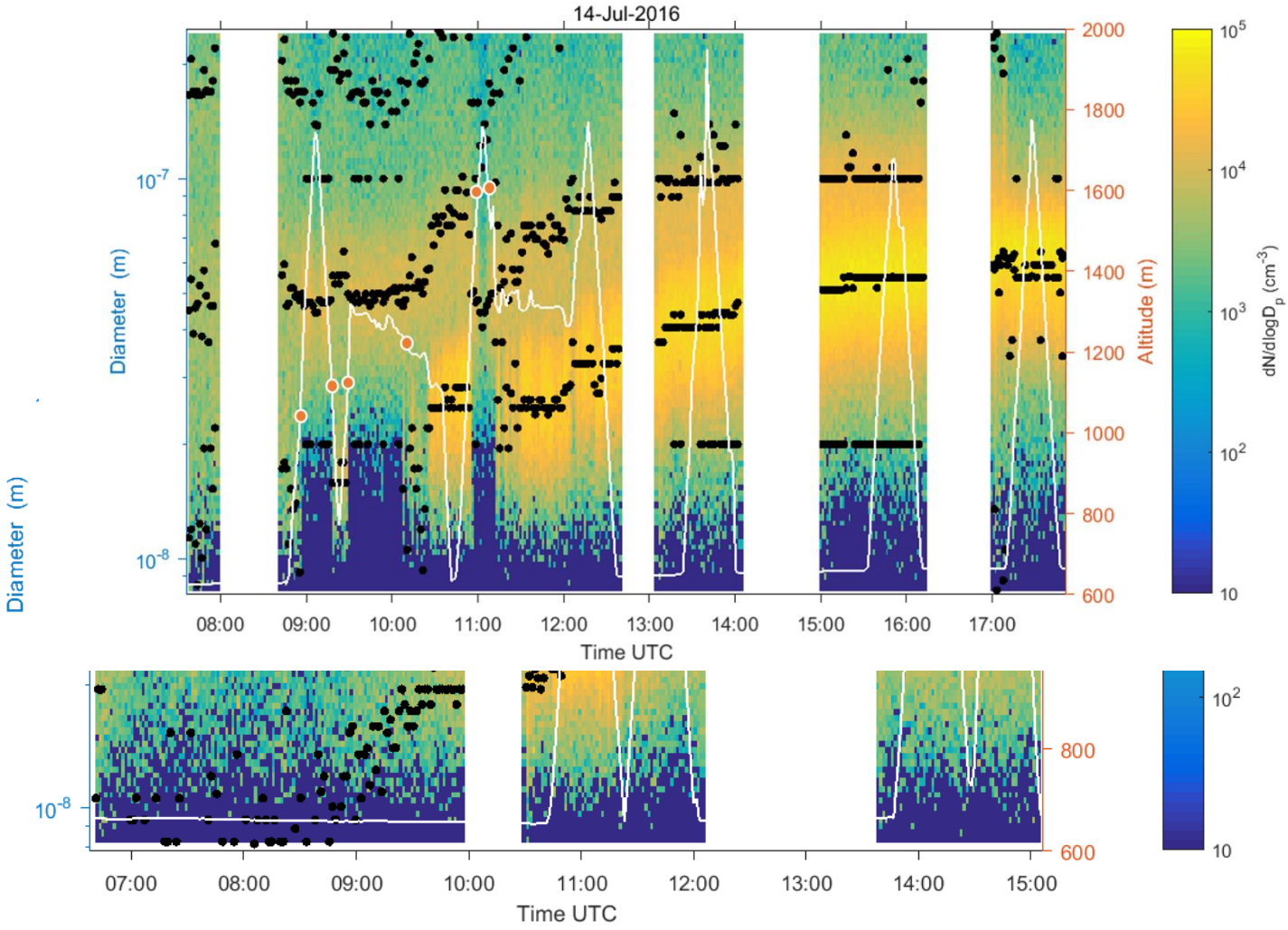


Figure 6

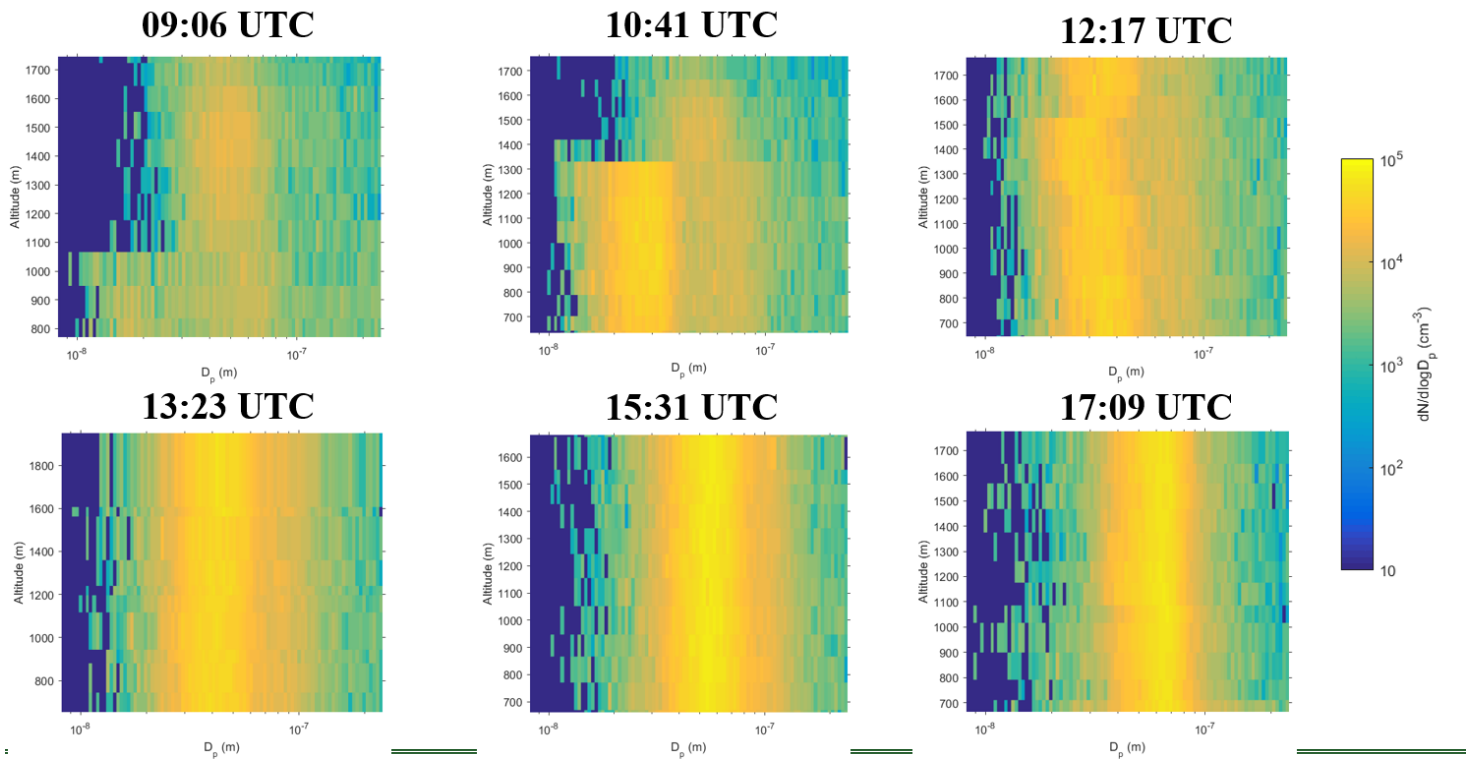


~~Figure 10~~

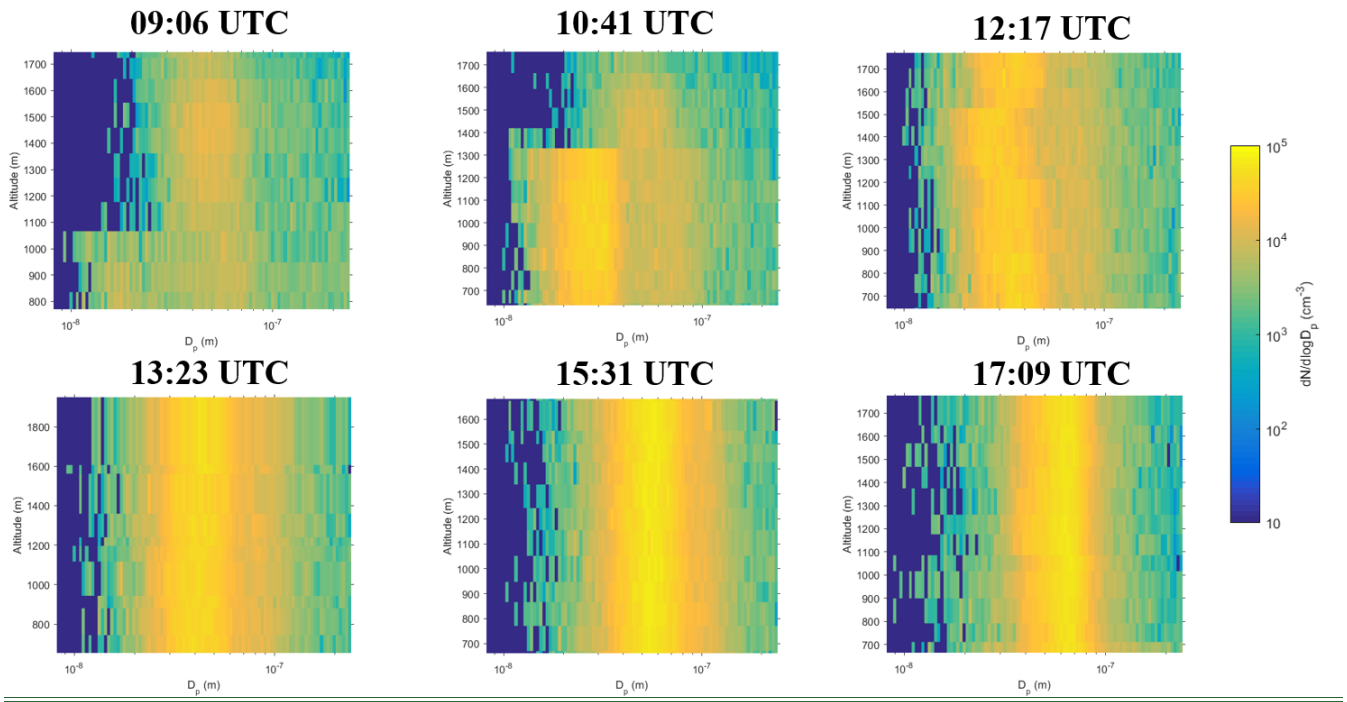


Figure 7

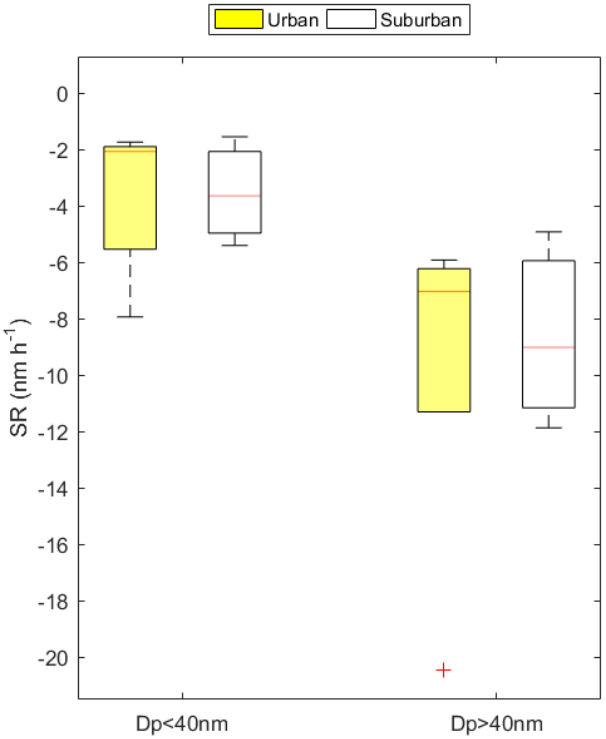


Figure 28

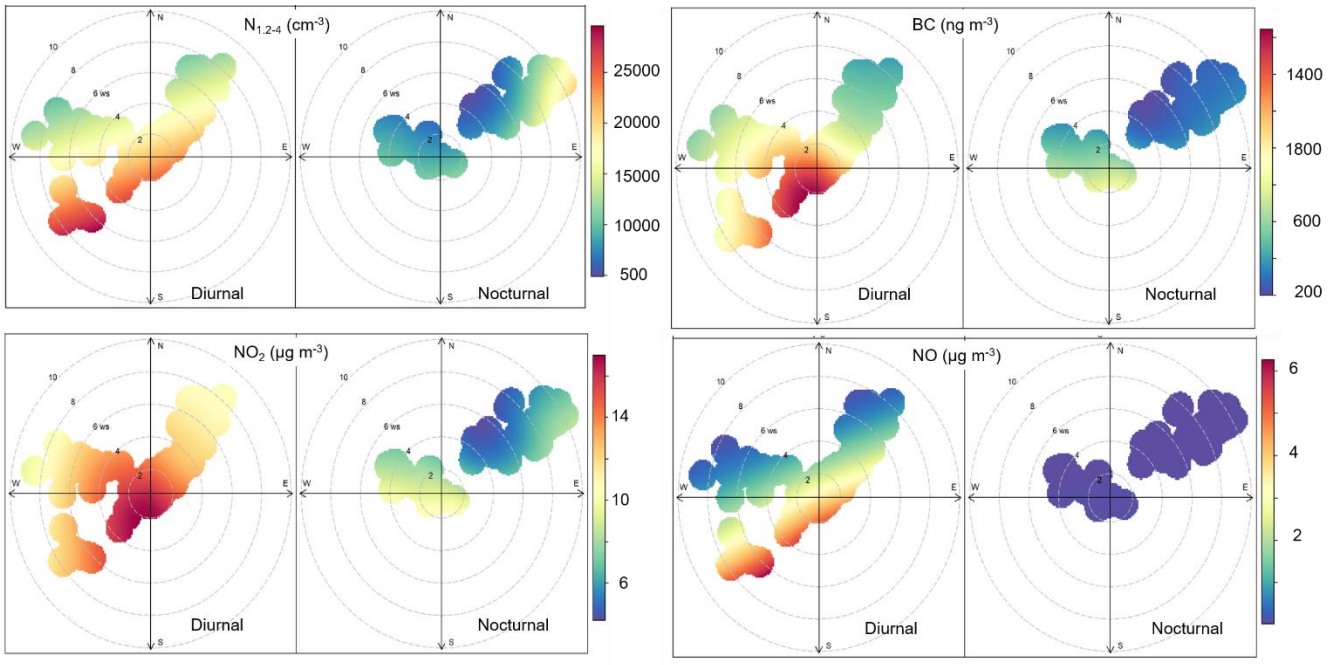


Figure 9